Chapter 3

G. Dietler and A. Haeberli,

–643.
.com, www.biosensingusa.com,
:ichertai.com/, www.plasmonic.
w.sensia.es, www.k-mac.co.kr/,
ɔchemie. nl, www.thermo.com,
:om, www.genoptics-spr.com,
www.graffinity.com, www.ibis-

:e, SPR pages http://www.

ıl. Chem., 2001, **73**, 5525–5531.
ɔpy, 2003, **57**, 320A–332A.
ey Dis., 2001, **38**, 481–487.
D. Areskoug and J. Buijs,

ıit., 2006, **19**(6), 478–534.
., 2007, **361**, 1–6.

CHAPTER 4

Kinetic Models Describing Biomolecular Interactions at Surfaces

DAMIEN HALL[1,a,b,c]

[a] University Chemical Laboratory, University of Cambridge, Lensfield Road, Cambridge CB2 1EW, UK; [b] Institute for Protein Research, Osaka University, 3-2 Yamadaoka, Suita, Osaka 565-0871, JAPAN; [c] Graduate School of Bioscience and Biotechnology, Tokyo Institute of Technology, B-39, 5249 Nagatsuta, Midori-ku, Yokohama 226-8501, JAPAN

4.1 Introduction

To say that the adsorption of molecules from solution to a surface is an important phenomenon in biochemistry is to make a major understatement. Indeed, so much of the fundamental chemistry of life occurs at interfacial regions [1–12] (Table 4.1) that the biochemists or biophysicists who take their subject seriously are required to have both an adequate understanding of how these processes occur and how they might be measured experimentally. The major thrust of this volume is concerned with interrogating the adsorption of biologically important molecules to surfaces by the use of optical biosensor technology. In this chapter, we discuss adsorption events from the perspective of monitoring a measurement signal which provides information, in real time, on the extent of solute adsorption to a surface. As discussion of time-dependent adsorption phenomena necessitates the use of kinetic models, we spend our time reviewing kinetic models that describe a wide range of adsorption behavior. We begin, however, by introducing the terminology of adsorption so that we might have the necessary language with which to conduct a discussion of the subject.

[1] Present address: Hall Laboratory. Institute for Basic Medical Sciences. Tsukuba University. 1-1-1 Tennoudai, Tsukuba, Ibaraki, 305-8575, JAPAN.

Table 4.1 Role of Adsorption in Fundamental Life Processes.

Biological Function	*Role of Adsorption*
Intra/Extra-Cellular Trafficking	First step in transfer of individual molecules and molecular complexes between various compartmentalized structures of the cell [1]. Also involved in transport to and from the cell *e.g.* pinocytosis and exocytosis [2].
Cell Signalling	Cell to cell communication is important both for single cell [3] and multi-cellular organisms [4]. Communication during such processes as tissue development is mediated by adsorption of specific signalling molecules to receptors located at the cell membrane surface [5].
Olfactory/Taste Senses	Initial step in sensory pathways of taste and smell involve adsorption of specific ligands to specific taste or smell receptors located on the cell surface [6,7].
Neuronal Impulse Transmission	Transmission of nerve impulses across synapses involves release of neurotransmitters from one side of the synaptic cleft and their subsequent adsorption to receptors on the opposing face of the synaptic cleft [8].
DNA Transcription RNA Translation	Transcription of DNA and translation of RNA involve adsorption of specific protein complexes to the one dimensional adsorptive surface of the nucleic acid polymer chain [9].
Immune Response	The first step in the defence against invading foreign agents involves adsorption of antibodies to the invading agent. The foreign agent constitutes an adsorptive surface composed of matrix sites termed epitopes that are specifically recognised by various immunoglobulin molecules [10].
Artificial Implant Technology	Material introduced into the body *e.g.* artificial joints, contact lenses, slow release drug reservoir *etc.* should have minimal potential to act as an adsorptive surface. Reduction of non-specific adsorption to various implant devices is an active area of research [11,12].

4.1.1 Terminology of Adsorption

In any solution-based adsorption experiment, one wishes to monitor the adsorption of a certain molecule in solution, termed the solute (or alternatively analyte), to the surface of a solid phase. The solid-phase adsorptive surface is composed of a number of sites that exert an attractive force for the solute. Once adsorbed to the surface the solute is termed the *adsorbate*. However, the term solute and adsorbate refer to any molecule that will bind to the surface specifically or non-specifically. Adsorption experiments are generally preceded by the preparation of a suitable adsorptive surface that is composed of a number of *binding sites* (alternatively known as matrix sites or immobilized ligand binding sites). The type of adsorptive surface that is prepared is necessarily dependent upon the system that is being studied however we might make a distinction as to the general type of surface in relation to a specific solute as constituting either a *distinct array* of binding sites or an effective *continuum* of binding sites (Figure 4.1). As a general rule, we may consider the adsorbing

ıal molecules and molecular
compartmentalized structures of
ransport to and from the cell *e.g.*
?].
ıportant both for single cell [3]
[4]. Communication during such
ent is mediated by adsorption of
to receptors located at the cell

of taste and smell involve
s to specific taste or smell
surface [6,7].
across synapses involves release
ıe side of the synaptic cleft and
o receptors on the opposing face

slation of RNA involve
ı complexes to the one
ce of the nucleic acid polymer

inst invading foreign agents
dies to the invading agent. The
ıdsorptive surface composed of
hat are specifically recognised
nolecules [10].
ly *e.g.* artificial joints, contact
voir *etc.* should have minimal
ive surface. Reduction of non-
implant devices is an active area

ne wishes to monitor the
d the solute (or alternatively
-phase adsorptive surface is
ve force for the solute. Once
lsorbate. However, the term
t will bind to the surface
ıents are generally preceded
ace that is composed of a
natrix sites or immobilized
ce that is prepared is neces-
ied however we might make
lation to a specific solute as
or an effective *continuum* of
ıay consider the adsorbing

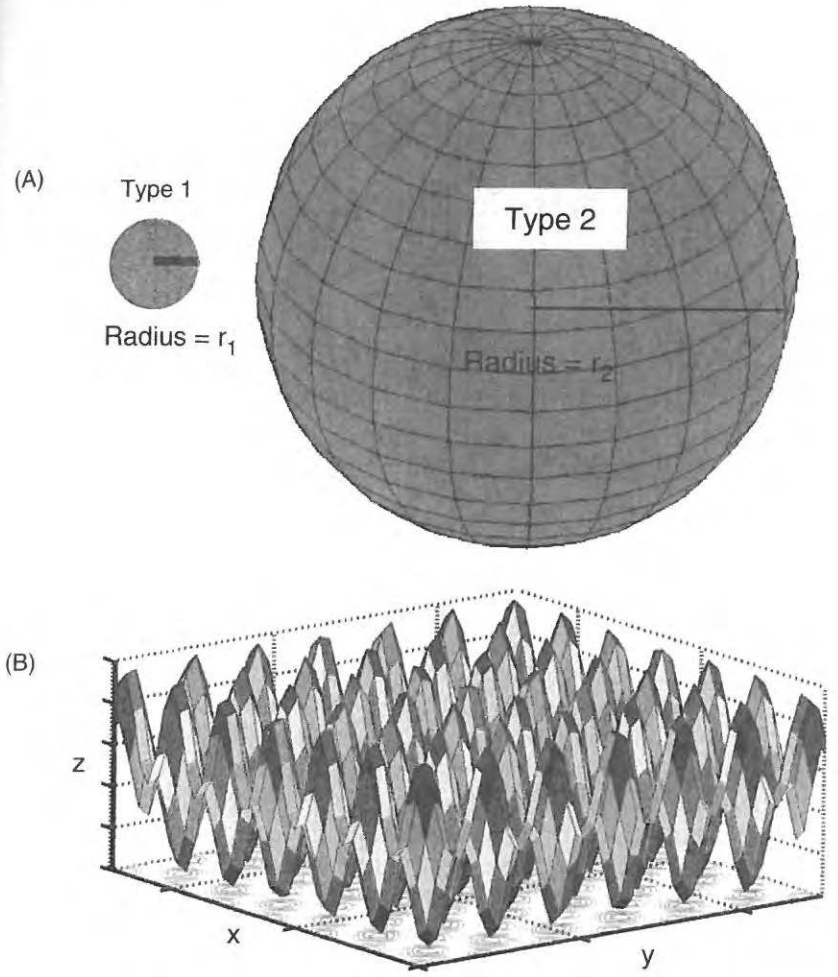

Figure 4.1 (A) The radius r of idealized spherical solute molecules (shown in green) may be small (r_1) or large (r_2) in relation to the distance between the adsorption sites on the adsorptive surface. (B) Diagram indicating a two-dimensional surface (surface plane). Colors indicate change in potential energy associated with the normal position of the center of the solute molecule from a distance r to $r+\Delta z$ away from the surface plane. Regions of lowest potential (blue) indicate position of adsorption sites. For adsorption of type 1 solute this two-dimensional adsorptive surface would constitute a distinct array. For adsorption of type 2 solute the surface would constitute a near continuum array. (C) Diagram indicating a three-dimensional adsorptive phase positioned at the interfacial boundary of the solid and liquid phases. Regions of low potential energy for solute (adsorption sites) are indicated by blue spheres. The supporting phase (often a polymer gel) is shown by red rods. As with the surface plane shown in (B), this surface phase may exist as either a distinct array or a near continuum array depending upon the dimensions of the adsorbing solute.

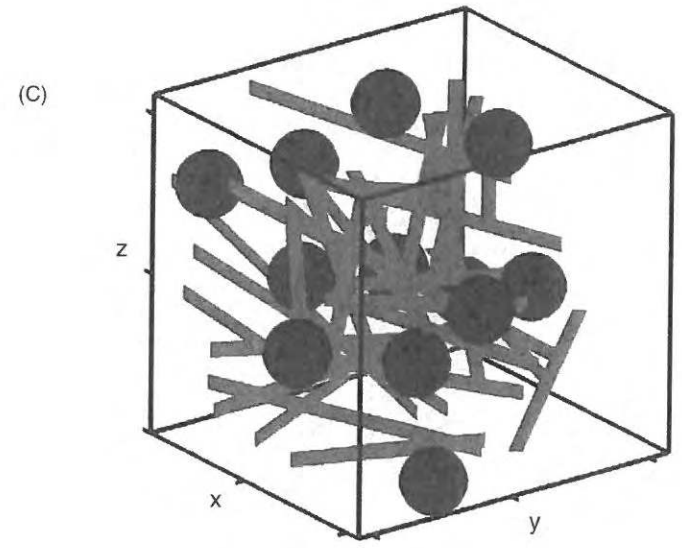

Figure 4.1 Continued

surface as a distinct array of sites if an adsorbate molecule, once bound, does not interfere with the subsequent adsorption of solute to any neighboring sites.

Once the adsorptive surface has been constructed, an *adsorption experiment* may be conducted by exposing this surface to a solution containing solute. Once introduced to the surface the solute will begin to adsorb[2] – a process which will continue until an *equilibrium* position is reached between the concentration of solute and the concentration of adsorbate. At this point, the process of adsorbate *desorption* may be studied by replacing the liquid phase with a solution not containing solute and recording the *dissociation* of adsorbate until an equilibrium ratio between solute and adsorbate is achieved. These basic adsorption and desorption experiments can be performed at different concentrations of added solute/initial adsorbate to examine the effect of concentration on the time-dependent (Figure 4.2a) or time-independent (Figure 4.2b) adsorption/desorption processes. Evaluation of the concentration dependence of the kinetic and equilibrium situations allows for the evaluation of the *rate* and *equilibrium constants* that define the behavior of the interaction under the particular conditions chosen for the study. These experiments may be repeated under different conditions in which a single environmental variable (*e.g.* temperature, pressure or composition of the buffer) is systematically altered to examine how the rate and equilibrium constants that define the adsorption event respond to the imposed change.

Until relatively recently with the experimental interrogation of solute adsorption from solution was made indirectly, using measurement strategies

[2] The particular forces that drive adsorption are outside the scope of this discussion.

ate molecule, once bound, does
f solute to any neighboring sites.
ucted, an *adsorption experiment*
o a solution containing solute.
ll begin to adsorb[2] – a process
sition is reached between the
of adsorbate. At this point, the
d by replacing the liquid phase
rding the *dissociation* of adsorb-
nd adsorbate is achieved. These
can be performed at different
bate to examine the effect of
ıre 4.2a) or time-independent
Evaluation of the concentration
ations allows for the evaluation
the behavior of the interaction
tudy. These experiments may be
a single environmental variable
of the buffer) is systematically
rium constants that define the
ge.
nental interrogation of solute
, using measurement strategies

he scope of this discussion.

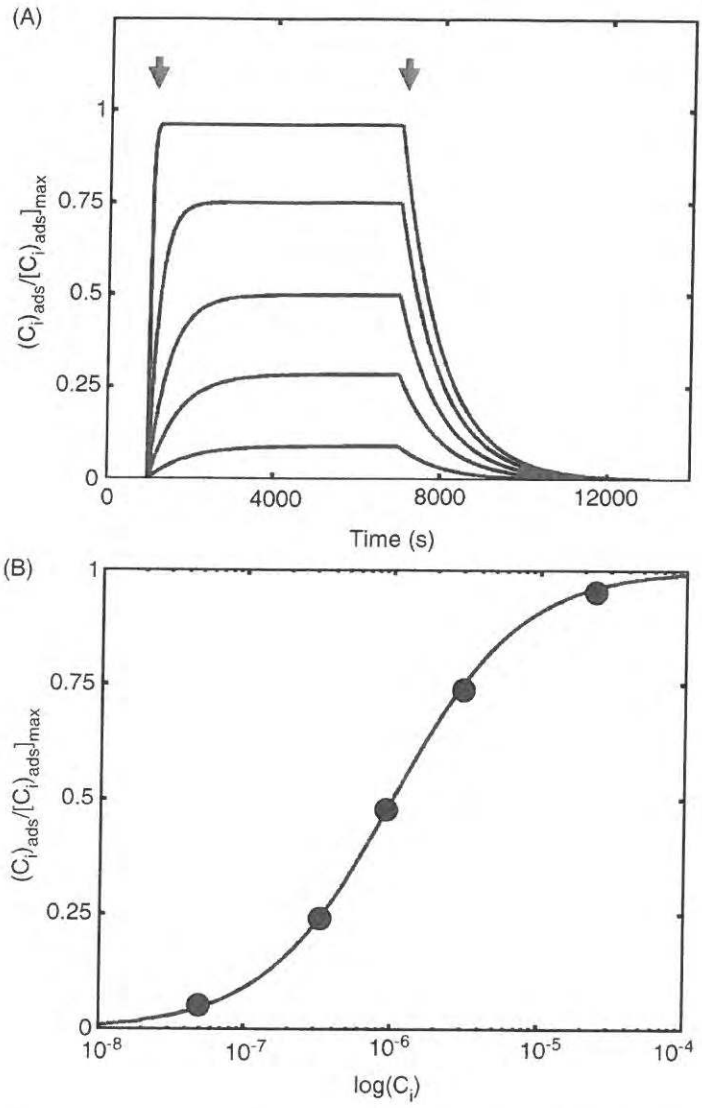

Figure 4.2 (A) Generalized profile of a time-dependent adsorption experiment: normalized concentration of adsorbate *vs.* time *t*. The first arrow shows the point of introduction of the solute to the adsorptive surface. In the association phase solute will continue to adsorb to the surface until an equilibrium is attained. The second arrow shows the point at which the liquid phase is replaced by buffer not containing solute. In this dissociation phase, adsorbate is allowed to dissociate from the surface until a new equilibrium position is reached. The five lines represent experiments carried out at five different concentrations. (B) General profile of a time independent adsorption experiment: the time independent values attained at the finish of each of the kinetic adsorption experiments are plotted against the equilibrium concentration of solute in the liquid phase.

based on difference measurements of the amount of solute depleted from the liquid phase [13]. Such indirect measurement strategies placed a limit on both the type of adsorption processes that could be studied and the temporal resolution with which that process could be resolved. The recent development of new techniques [14,15] allows for direct measurement of the amount of adsorbed solute and has afforded a time resolution that is almost contemporaneous with the adsorption event. Of these new techniques, those based on evanescent wave optical biosensor technology [16–18] have become the most popular, mainly due to the successful commercialization of the technology.

4.1.2 Optical Quantification of Adsorption at an Interface

Evanescent wave optical biosensor technology is reliant upon the physics of the total internal reflection (TIR) of light. Light shone at an interface[3] below a certain critical angle will enter the second medium and be refracted by it to an extent governed by the refractive indices of the two mediums [19]. At incident angles greater than the critical angle, the light will not enter the second optical medium but will instead be totally internally reflected back into the first medium. The electric and magnetic fields associated with the reflected ray of light, however, do not end abruptly at the point of reflection but will penetrate somewhat into the second medium. Interaction of these decaying electric and magnetic fields (termed evanescent fields) with the second medium beyond the interfacial plane will subtly change the properties of the reflected beam. The degree of non-absorptive interaction of the electrical component of the evanescent light with the matter at the interfacial region will be determined by the electrical polarizability of the material at the interface. Thus, optical biosensor technology can be taken to reflect changes in refractive index at the interfacial layer.[4] The field strength associated with the evanescent light at the interface decays exponentially with distance normal to the surface, z, making the observed signal, S, proportional to refractive index changes very close to the surface [eq. (4.1)].

$$S \propto \int_0^\infty \Delta n(z) \exp(-z/\sigma) \mathrm{d}z \tag{4.1}$$

The parameter σ is the field strength decay constant and has units of distance. For planar surfaces it is typically of the order of 0.3–0.5 times the wavelength of the light used in the TIR experiment [19]. For a wide range of substances[5] the change in refractive index in response to varying the weight concentration of

[3] An interface existing between two optically transparent mediums.
[4] For optically transparent materials, the macroscopic quantity related to the electrical polarizability is the refractive index.
[5] The approximate dn/dc values for proteins and nucleic acids are 0.18 and 0.16 ml g^{-1}, respectively. The values for different types of carbohydrate range from 0.10 to 0.18 ml g^{-1}.

ɔunt of solute depleted from the
strategies placed a limit on both
ɪ be studied and the temporal
ɛsolved. The recent development
measurement of the amount of
ɹlution that is almost contempo-
new techniques, those based on
/ [16–18] have become the most
ɛialization of the technology.

ption at an Interface

is reliant upon the physics of the
shone at an interface[3] below a
ium and be refracted by it to an
e two mediums [19]. At incident
will not enter the second optical
ly reflected back into the first
ɔciated with the reflected ray of
ɪt of reflection but will penetrate
n of these decaying electric and
the second medium beyond the
rties of the reflected beam. The
lectrical component of the eva-
region will be determined by the
ɪterface. Thus, optical biosensor
efractive index at the interfacial
ɛvanescent light at the interface
to the surface, z, making the
index changes very close to the

$z/\sigma)\mathrm{d}z$ (4.1)

nstant and has units of distance.
`0.3–0.5 times the wavelength of
a wide range of substances[5] the
ing the weight concentration of

mediums.
ɪantity related to the electrical polariz-

acids are 0.18 and 0.16 ml g^{-1}, respec-
ge from 0.10 to 0.18 ml g^{-1}.

component i, c_i, can be approached as a linear function as the derivative $\mathrm{d}n/\mathrm{d}c_i$ is approximately constant [eq. (4.2)].

$$n(c_i) = n(c_i = 0) + \left(\frac{\mathrm{d}n}{\mathrm{d}c_i}\right)c_i \tag{4.2}$$

Substitution of eq. (4.2) into eq. (4.1) allows us to relate the change in signal, ΔS, for situations in which initially no component i is present ($c_i = 0$), with changes in the weight concentration of component i at the interfacial layer [eq. (4.3)].

$$\Delta S \propto \frac{\mathrm{d}n}{\mathrm{d}c_i}\int_0^\infty \frac{\mathrm{d}c_i}{\mathrm{d}z}\exp(-z/\sigma)\mathrm{d}z \tag{4.3}$$

On the basis of eq. (4.3), we can appreciate that the measured signal is, strictly, not a linear descriptor of the concentration of adsorbate but for many cases it will very nearly be so. Figure 4.3 describes the apparent change in signal that would be registered for a constant mass of adsorbate in a number of different modes of adsorption on the surface of an optical biosensor. On the basis of eq. (4.3), the relative signal (normalized to the type 1 case) for each adsorption mode would be type 1, 1; type 2, 1.01; type 3, 0.56; and type 4, 0.23.

A variety of ingenious means (of which SPR [20] is perhaps the best known) have been developed to maximize the changes in the reflected beam of light so as to make it a viable means for experimental measurement. Although the physics of each different experimental detection method differ somewhat, all optical biosensor technology share basic characteristics as outlined in eqs. (4.1)–(4.3). More is said about the physics and instrumentation particular to SPR in Chapters 2 and 3. For the remainder of the current chapter we will discuss kinetic models that are relevant to different aspects of the process of adsorption as studied by optical biosensor technology. Although we will not specifically transform the concentration units of the adsorption profile into an equivalent signal as defined by eq. (4.3), we ask the reader to keep in mind the likely consequences of the transformation for some of the more complicated adsorption geometries.

4.2 Defining Factors of the Adsorption Event

For adsorption to occur two events must happen in sequence: first the solute must be transported to the surface, and second the solute must successfully interact with the surface to form the adsorbate. We will discuss each of these events in greater detail in subsequent sections; however, a basic understanding of the distinction between the two regimes can be gained by casting the adsorption event in terms of a simple transport/reaction process [21] [eq. (4.4)].

$$C_i \underset{k_b}{\overset{k_a}{\rightleftharpoons}} \{C_i\} \underset{k_2}{\overset{k_1'}{\rightleftharpoons}} (C_i)_{\mathrm{ads}} \tag{4.4}$$

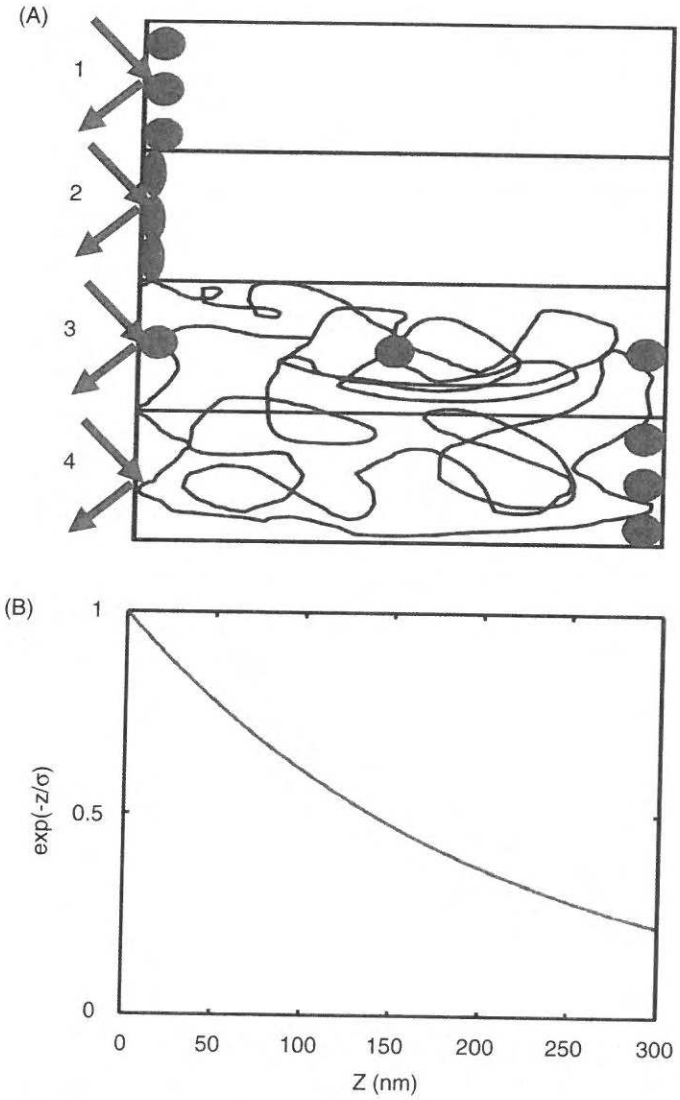

Figure 4.3 (A) Four different modes of solute adsorption with the adsorptive surface at which the light is totally internally reflected shown on the vertical left axis. Type 1 adsorption: the solute adsorbs directly on the surface plane and maintains its shape. Type 2: the solute adsorbs and undergoes a post-adsorption isomerization to maximize its interaction with the surface. Type 3: the solute adsorbs to matrix sites on a supporting polymer molecule in an evenly dispersed manner. Type 4: the solute adsorbs on a supporting polymer molecule preferentially on the bulk solution side. On the basis of eq. (4.3), the relative signal (normalized to the type 1 case) for each adsorption mode would be type 1, 1; type 2, 1.01; type 3, 0.56; and type 4, 0.23. (B) The decrease in evanescent field strength with distance normal to the surface for a decay constant $\sigma = 200\,\text{nm}$ (approximate case for light used in TIR experiment of wavelength 600 nm).

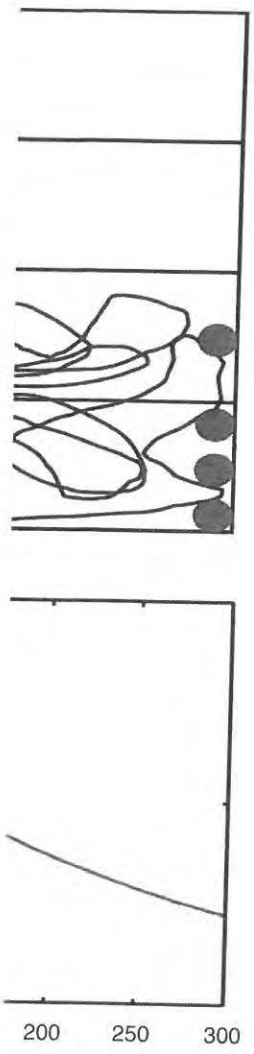

rption with the adsorptive surface
flected shown on the vertical left
rbs directly on the surface plane
ite adsorbs and undergoes a post-
its interaction with the surface.
sites on a supporting polymer
. Type 4: the solute adsorbs on a
lly on the bulk solution side. On
normalized to the type 1 case) for
1; type 2, 1.01; type 3, 0.56; and
scent field strength with distance
nt $\sigma = 200$ nm (approximate case
elength 600 nm).

In this formulation, C_i, $\{C_i\}$ and $(C_i)_{ads}$ represent the concentration of solute of type i, the concentration of solute of type i spatially close to the surface (termed intimate solute) and the concentration of adsorbed solute of type i (the adsorbate), respectively. Equation (4.4) describes the process whereby solute approaches and leaves the surface at a rate defined by phenomenological transport coefficients k_a and k_b. Once in physical proximity to the surface, the intimate solute may react to form adsorbate according to an association rate function k_1' and a reverse rate constant k_2, where both k_1' and k_2 have units of s^{-1}. In the simplest instance the association rate function may be further decomposed [eq. (4.5)] into an intrinsic second-order rate constant k_1, the initial total concentration of matrix sites,[6] $(C_x)_{tot}$ and some unitless function describing the surface site occupation, $f(\phi)$, where $\phi = n(C_i)_{ads}/(C_x)_{tot}$ (n is the average number of sites covered by the adsorbed solute). More will be said about the surface function, but for now we may treat $f(\phi)$ as describing the fraction of total matrix sites available for participation in further adsorption of solute.

$$k_1' = k_1(C_x)_{tot} f(\phi) \tag{4.5}$$

In the simple scheme set forth in eq. (4.4), the rate of formation of the intimate solute is given by eq. (4.6).

$$\frac{d\{C_i\}}{dt} = k_a C_i - k_b\{C_i\} - k_1'\{C_i\} + k_2(C_i)_{ads} \tag{4.6}$$

The so-called transport-limited case represents the situation in which the rate of physical encounter between solute and surface dictates the rate of formation of the adsorbate species. This situation occurs for non-equilibrium cases when $[k_1'\{C_i\} - k_2(C_i)_{ads}] \gg [k_a C_i - k_b\{C_i\}]$, making the rate of formation of the intimate solute effectively zero ($d\{C_i\}/dt \to 0$). It results in the effective association rate being given by eq. (4.7a). In the limit of zero adsorbate concentration, $(C_i)_{ads} \approx 0$, the effective forward rate parameter f_i, can be approximated by a ratio of reaction and transfer rate constants with the further approximation for f_i allowable if the transport coefficient is much smaller than the reaction rate ($k_b \ll k_1'$) [eq. (4.7b)]. In the alternative limit of zero solute concentration, $C_i \approx 0$, the effective dissociation rate parameter b_i is given by eq. (4.7b), again with the additional approximation valid if $k_b \ll k_1'$ (here $K_R' = k_1'/k_2$). For a given degree of surface occupation an effective adsorption partition constant

[6] To speak of a total concentration of adsorption sites one must assign a reaction volume to the surface and treat the adsorbed layer as a three-dimensional phase. An alternative treatment is to consider the surface layer as a two-dimensional plane with adsorbate and binding site concentrations given in terms of mol m^{-2}. This results in the usual set of units. This results in an unusual set of units for the resulting equilibrium ($m^3\ mol^{-1}$) and association rate constants ($m^3\ mol^{-1}\ s^{-1}$). We prefer the former treatment as it is conceptually similar to solution chemical kinetics. Despite the differences, the two treatments are formally equivalent.

(unit-less) can then be determined by the ratio of effective forward and reverse rate parameters $[(K_i)_{\text{eff}} = f_i/b_i]$ (Eq. 4.7b).

$$\frac{d(C_i)_{\text{ads}}}{dt} = k_1' \left[\frac{k_a C_i + k_2 (C_i)_{\text{ads}}}{k_b + k_1'} \right] - k_2 (C_i)_{\text{ads}} \tag{4.7a}$$

$$\therefore f_i \approx \frac{k_1' k_a}{k_b + k_1'} \approx k_a;\ b_i \approx \frac{k_b k_2}{k_b + k_1'} \approx \frac{k_b}{K_R'};(K_i)_{\text{eff}} = \frac{k_1' k_a}{k_2 k_b} \tag{4.7b}$$

In the antithetical, reaction-limited kinetic regime $[k_1'\{C_i\} - k_2(C_i)_{\text{ads}}] \ll [k_a C_i - k_b\{C_i\}]$, the concentration of intimate solute is little perturbed by the reaction component of eq. (4.6), allowing a quasi-equilibrium approximation such that $\{C_i\} \approx (k_a/k_b)C_i = K_T C_i$ (where K_T represents an equilibrium partition constant for formation of the intimate solute) leaving the reaction rate to be written as eq. (4.8a). In this case, the effective association rate parameter, f_i, in the limit of zero adsorbate $[(C_i)_{\text{ads}} \approx 0]$ and the effective dissociation rate constant, b_i, in the limit of zero solute $(C_i \approx 0)$ and the effective adsorption partition constant, $(K_i)_{\text{eff}} = f_i/b_i$, can be described by eq. (4.8b).

$$\frac{d(C_i)_{\text{ads}}}{dt} = k_1' K_T C_i - k_2 (C_i)_{\text{ads}} \tag{4.8a}$$

$$\therefore f_i \approx k_1' K_T;\ b_i \approx k_2;\ (K_i)_{\text{eff}} = \frac{k_1' k_a}{k_2 k_b} \tag{4.8b}$$

Although we have presented the two extreme antithetical kinetics regimes the system under study may exhibit "mixed" kinetic behavior, in which case no simplifying relationship can be deduced and the numerical solution of two coupled differential equations [eqs. (4.6) and (4.9)] must be performed with the apparent phenomenological rate constants varying between the two limits set out in eqns. (4.7b) and (4.8b) depending on the relative concentrations of solute, sites for adsorption and adsorbate.

$$\frac{d(C_i)_{\text{ads}}}{dt} = k_1'\{C_i\} - k_2 (C_i)_{\text{ads}} \therefore k_a > f_i > k_1' K_T \quad \text{and} \quad \frac{k_b}{K_R'} > b_i > k_2 \tag{4.9}$$

4.2.1 Mass Transfer

In optical biosensors, the solute is introduced to the adsorptive surface in either a flow-through or a cuvette-type system. In the flow-through biosensor (Figure 4.4), the adsorptive surface constitutes the base of a microfluidic channel through which solution flows at some average velocity v^*. As the solute is taken up by adsorption it is replaced anew by solute flowing in from further down the channel. In the cuvette-type biosensor (Figure 4.5), the

of effective forward and reverse

$$\text{ads}\Big] - k_2(C_i)_{\text{ads}} \qquad (4.7a)$$

$$\frac{k_b}{K'_R};(K_i)_{\text{eff}} = \frac{k'_1 k_a}{k_2 k_b} \qquad (4.7b)$$

regime $[k'_1\{C_i\} - k_2(C_i)_{\text{ads}}] \ll$
solute is little perturbed by the
uasi-equilibrium approximation
resents an equilibrium partition
leaving the reaction rate to be
ssociation rate parameter, f_i, in
the effective dissociation rate
)) and the effective adsorption
ed by eq. (4.8b).

$$_2(C_i)_{\text{ads}} \qquad (4.8a)$$

$$\Gamma = \frac{k'_1 k_a}{k_2 k_b} \qquad (4.8b)$$

antithetical kinetics regimes the
tic behavior, in which case no
he numerical solution of two
9)] must be performed with the
ing between the two limits set
the relative concentrations of

$$K_T \quad \text{and} \quad \frac{k_b}{K'_R} > b_i > k_2 \qquad (4.9)$$

to the adsorptive surface in
In the flow-through biosensor
s the base of a microfluidic
e average velocity v^*. As the
new by solute flowing in from
e biosensor (Figure 4.5), the

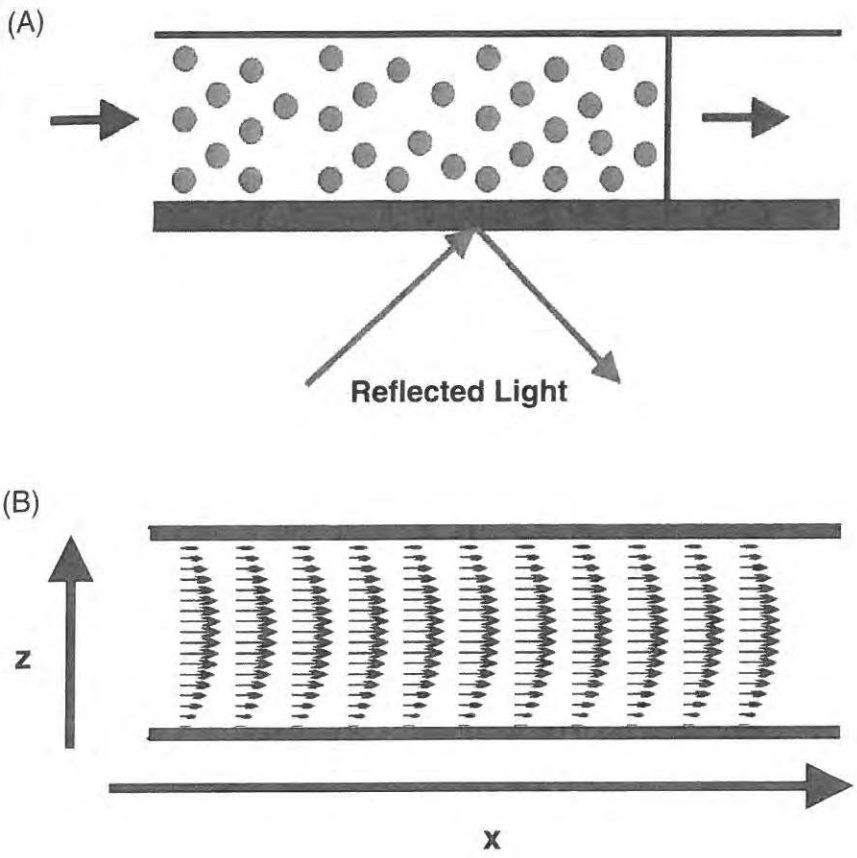

Figure 4.4 (A) Diagram depicting the general characteristics of a flow-through type biosensor. Solute is introduced as a plug into a microfluidic channel at controlled flow rate. The adsorptive surface at which light is totally internally reflected constitutes one side of the microfluidic channel. As solute is adsorbed to the surface, it is replaced by the solute flowing through behind allowing the liquid phase concentration for certain experimental regimes to be considered a constant. (B) Idealized representation of the velocity field associated with flow in an optical biosensor based on the parabolic flow assumption [eq. (4.12)].

adsorptive surface constitutes the base of a microcuvette into which solute is added. To effect efficient mass transfer, the solution is subjected to shear forces generated by aspiration cycles from a free wall jet device (see Chapter 3) or by a stirring rod suspended near the top of the solution.

The most general approach for describing the mass transfer process first involves the spatial discretization of the solution volume comprising the biosensor device, followed by numerical solution of a continuity equation (for the cases of non-turbulent flow [22] describing the diffusion, convection and

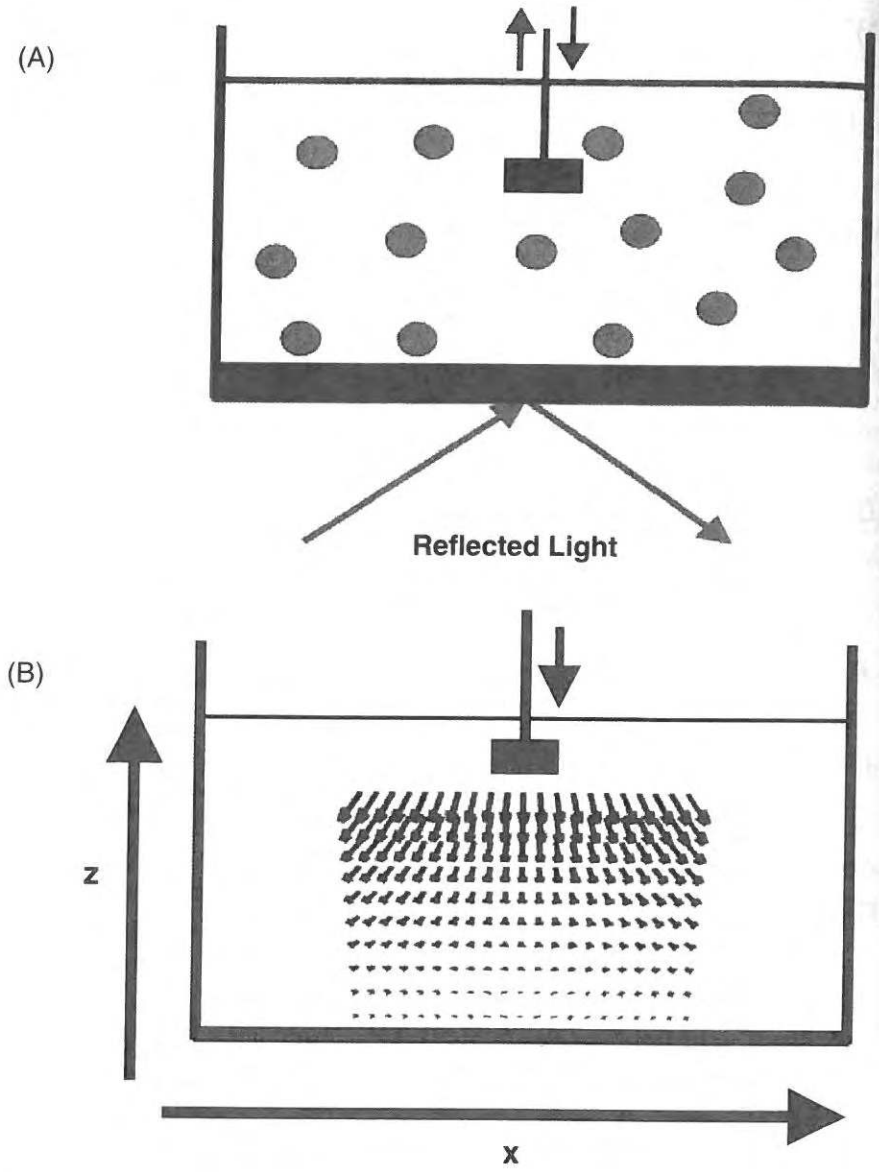

Figure 4.5 (A) Diagram depicting the general characteristics of a cuvette-type biosensor. Solute introduced by injection into an open cuvette is subjected to shear forces by an oscillating stirrer. The adsorptive surface at which light is totally internally reflected is positioned at the base of the cuvette. As the solute is adsorbed to the surface it is depleted from solution meaning that except for cases of insignificant depletion the solution phase concentration of solute must be calculated by difference between the total and adsorbed concentrations. (B) An idealized representation of the velocity field associated with stirring in a cuvette type optical biosensor based on the stagnant point flow assumption [eq. (4.13)].

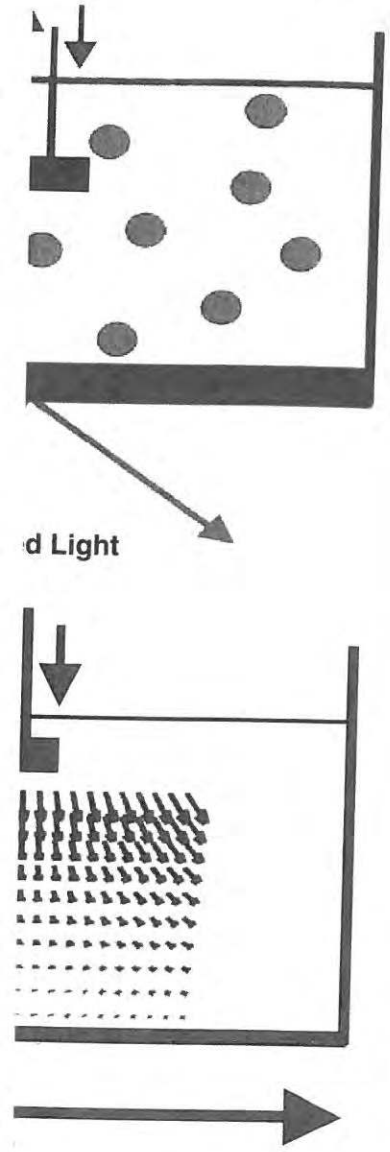

aracteristics of a cuvette-type bio-
into an open cuvette is subjected to
ne adsorptive surface at which light
ed at the base of the cuvette. As the
epleted from solution meaning that
on the solution phase concentration
ace between the total and adsorbed
sentation of the velocity field asso-
e optical biosensor based on the
.13)].

adsorption of the solute component) [eq. (4.10)]. Here D_i and v_i denote the solute's diffusion coefficient and linear velocity.[7,8,9]

$$\left(\frac{dC_i}{dt}\right) = \underset{\text{mass transport}}{\nabla(D_i \nabla C_i) - \nabla([C_i v_i])} \underset{\text{reaction}}{- k_1' C_i + k_2 (C_i)_{ads}} \tag{4.10a}$$

$$\frac{d(C_i)_{ads}}{dt} = k_1' C_i - k_2 (C_i)_{ads} \tag{4.10b}$$

For efficient mass transport, we require that, for points in close spatial proximity to the adsorptive surface, the absolute values of the mass transport term in eq. (4.10a) be either greater than the forward reaction term, for association experiments, or greater than, the reverse reaction term, for experiments examining dissociation of adsorbate.[10] From inspection of eq. (4.10a), we note that we may influence this ratio by changing the transport parameters D_i and v_i or alternatively modifying the reaction parameters C_i, $(C_x)_{tot}$ and $f(\phi)$ (the last two parameters housed in the association rate function k_1'). For a particular system of interest, one can usually vary C_i and $(C_x)_{tot}$ by careful experimental design leaving the transport parameters D_i and v_i as the important variables to be considered. With regard to the diffusion of solute, we note that D_i for a spherical solute of radius r_i existing in an aqueous solvent of viscosity η at temperature T can be written [23] as eq. (4.11):

$$D_i = \frac{kT}{6\pi\eta r_i} \tag{4.11a}$$

$$r_i = \sqrt[3]{\frac{3\bar{v}_i M_i}{4\pi N_A}} \tag{4.11b}$$

where k is Boltzmann's constant, N_A is Avogadro's number, $\bar{v}_i$ is the partial specific volume of the solute and M_i is the solute molecular weight. In the context of achieving efficient mass transfer in biosensor adsorption experiments, we are interested how D_i depends on the environmental variables of solution temperature and composition [24–27] (Table 4.2). With respect to temperature, we note that the viscosity of water (and dilute aqueous solutions) between temperatures of 0 and 50°C can be described very well by an empirical exponential dependence (where $\eta_{0°C\,(LIQUID)} = 1.8 \times 10^{-3}\,kg\,s^{-1}\,m^{-1}$), allowing an estimation[11] of the solute diffusion coefficient that shows a significant increase with temperature over this range.

[7] Eq. (4.10) must be appropriately modified for spatial boundary conditions, *i.e.* to account for the motion /reaction of solute at or near physical boundaries.

[8] The operator ∇ when applied to a function f, ∇f, implies the sum of spatial derivatives, *e.g.* $\partial f/\partial x + \partial f/\partial y + \partial f/\partial z$.

[9] The reaction component is presented as a simple mechanistically concerted process for simplicity. For sequential based reaction processes this must be modified.

[10] That is, $(dC/dt)_{reaction}/(dC/dt)_{transport} \to 0$.

[11] Valid for solutes that will not significantly change their average dimensions upon experiencing a change in temperature, *e.g.* as might a protein upon temperature-induced protein unfolding.

Table 4.2 Dependence of solute diffusion coefficient on solution parameters capable of variation in optical biosensor experimentation.

Particular Dependence	*Relevant equation describing diffusion coefficient*
Temperature (for Water) [24]	$D_i = \dfrac{kT}{6\pi\,[0.0018\exp(-0.0236(T-273.1))]\,r_i}$
Weight Concentration of viscogenic agent[i] [25] **(at 20°C)**	$D_i = \dfrac{kT}{6\pi\,[0.00103 + Ac_v + Bc_v]r_i}$
Concentration and dimensions of the supporting gel phase [26,27]	$D_i = (D_i)_{\varphi=0}\exp\left\{-\left(\dfrac{r_i}{\Delta r}\right)\sqrt{\varphi}\right\}$

[i] For glycerol, A = 2.18e-6, B = 9.0e-9, for sucrose, A = 1.11e-6, B = 1.96e-8.

With regard to the dependence of the solute diffusion coefficient on solution composition, the most pertinent changes for consideration are those due to the addition of viscogenic agents often required for biochemical stability, most commonly glycerol or sucrose [25], or those brought about by the use of a tethered polymer gel layer [26,27]. Table 4.2 describes the estimated diffusion coefficient for a spherical solute as a function of added glycerol or sucrose as viscogenic agents (designated c_v) at 20°C [25]. A common feature of optical biosensor experimentation is the use of a chemically inert tethered polymer support such as carboxymethyldextran to act as a point of covalent attachment for biological ligands [17,18]. Over a small distance scale the tethered polymer support has the potential to act as a porous chemical phase acting to retard diffusion of the solute in a size dependent manner. A simple estimate[12] of the potential for reduction in diffusion coefficient of a spherical solute's diffusion coefficient upon entering a porous gel has been provided by Ogston *et al.* [26,27]. They treated the polymer phase as a randomly arranged collection of very long cylindrical rods having a radius Δr and a fractional volume occupation φ. Using this approach, one may estimate the dependence of the diffusion coefficient of a spherical solute on the size of solute and the concentration of rod like polymer[13] constituting the gel phase $D_i(r_i, \varphi)$ as shown in Table 4.2.

Although reasonable estimates of the diffusion coefficient[14] can be gained from experiment or theory, estimation of the velocity profile for a particular configuration requires detailed device dimensions as input parameters in simulations based on the Navier–Stokes equations [28,29]. However, some general conclusions can be made about the velocity profiles operating in flow-through

[12] With some experimental support.
[13] Yarmush *et al.* [32] have additionally raised the possibility that the diffusion coefficient of solute in the gel will be sensitive to changes in the concentration of adsorbate. This will have the effect of decreasing the rate of mass transfer to lower regions of the gel in an occupancy-dependent manner.
[14] Diffusion is assumed isotropic.

coefficient on solution parameters
biosensor experimentation.

on describing diffusion coefficient
$\frac{kT}{\exp(-0.0236(T-273.1))]\, r_i}$
$\frac{kT}{3+Ac_v+Bc_v]r_i}$
$p\left\{-\left(\frac{r_i}{\Delta r}\right)\sqrt{\varphi}\right\}$

: 1.11e-6, B = 1.96e-8.

ite diffusion coefficient on solution
consideration are those due to the
d for biochemical stability, most
e brought about by the use of a
! describes the estimated diffusion
on of added glycerol or sucrose as
25]. A common feature of optical
chemically inert tethered polymer
as a point of covalent attachment
istance scale the tethered polymer
s chemical phase acting to retard
anner. A simple estimate[12] of the
it of a spherical solute's diffusion
been provided by Ogston *et al.*
randomly arranged collection of
and a fractional volume occupa-
te the dependence of the diffusion
f solute and the concentration of
$D_i(r_i, \varphi)$ as shown in Table 4.2.
usion coefficient[14] can be gained
e velocity profile for a particular
sions as input parameters in sim-
ns [28,29]. However, some general
profiles operating in flow-through

ility that the diffusion coefficient of solute
n of adsorbate. This will have the effect of
he gel in an occupancy-dependent manner.

biosensor designs and in cuvette-type biosensor designs by assuming idealized velocity profiles that are related to simpler cases.[15] For the flow-type biosensor, one approach has been to treat the problem as flow in an open-ended pipe and hence describe the velocity profile [30–34] as the simple parabolic type (Figure 4.4b) where the linear velocity in the x direction, v_x, is expressed as a function of position of the height of the channel, z, which has a maximum height of z_{max} [eq. (4.12)].

$$v_x(z) = 4v_x(z_{max}/2)\left(\frac{z}{z_{max}} - \frac{z^2}{z_{max}^2}\right) \tag{4.12}$$

As can be noted from Figure 4.4b, the linear x component of the velocity of solute i approaches zero at the channel walls and is maximal in the central region. Simple approximate models for predicting the velocity profile are harder to come by for the cuvette-type biosensor because stirring is carried out differently in different machine types. However, some information can be gained from a limiting case analysis in terms of the stagnation point flow assumption in a stirred cuvette [35,36]. In this treatment, a reduced subsection of the flow profile is regarded as emanating from the position of the stirrer bar and is expected to disperse symmetrically as it approaches the surface (leaving a so-called "stagnant point" on the adsorptive surface in the area immediately below the point of stirring and a stagnant flow region next to the surface) [Figure 4.5b and eq. (4.13)].

$$v_x = 0.164B^{\frac{3}{2}}\left(\frac{\eta}{\rho}\right)^{-\frac{1}{2}} xz \tag{4.13a}$$

$$v_z = 0.164B^{\frac{3}{2}}\left(\frac{\eta}{\rho}\right)^{-\frac{1}{2}} z^2 \tag{4.13b}$$

In these equations, B is a multi-term flow constant, dependent on device geometry for which values can be found in Ref. [35] and references therein. With regard to coordinate position, the point of origin is the point on the surface immediately below the stirring device. As with the parabolic flow assumption in the flow-through device, the predicted velocity for the cuvette device approaches zero at the surface.

The full numerical solution of the continuity equation ([eq. (4.10)] can be a daunting task. However, nearly all problems involving mass transfer to a surface may, with varying degrees of success, be decomposed into simpler compartment models [34,37,38] (Figure 4.6) reminiscent of the descriptive model outlined in eq. (4.4). The basis of the two-compartment simplification

[15] Here we consider convective flow up to the plane of the adsorptive surface. For situations where the adsorption sites are attached to a polymer gel layer we assume that the polymer layer will disturb flow and consider the surface of the tethered polymer layer as the relevant surface for defining the velocity profile. Some authors also have considered the penetration of flow into any such gel layer [39].

lies in the observation (noted above for the stagnant point flow and the parabolic flow cases) that the velocity profile of a fluid flowing over a stationary surface approaches zero at the limit of contact with the surface (*i.e.* $z=0$). This zero flow region or stagnant layer may be considered as extending out a small distance, δ, from the surface. A neighboring similar-sized region beyond this distance δ, termed the bulk, is considered to move

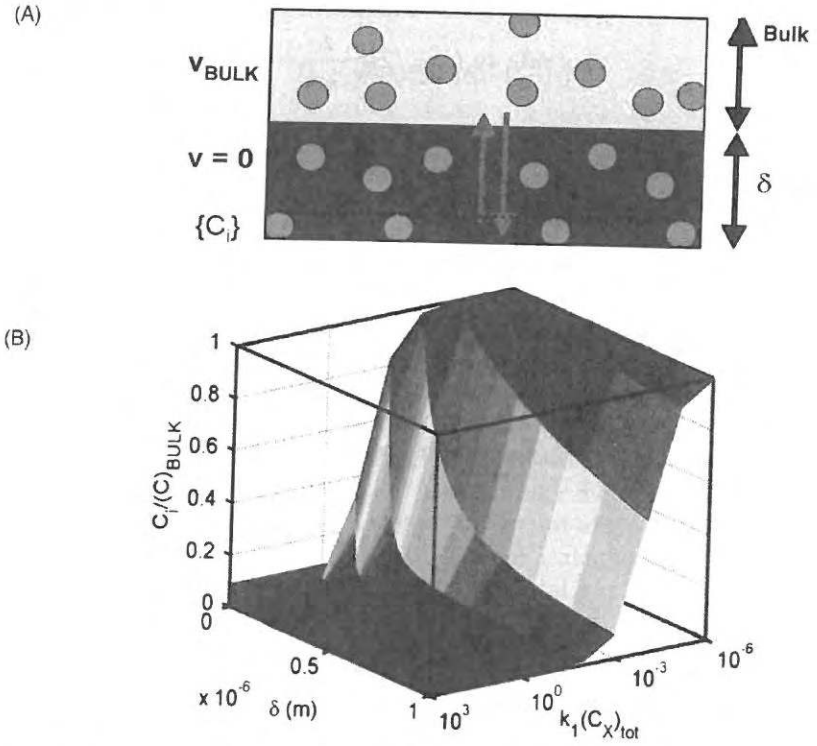

Figure 4.6 (A) Two-compartment model for describing mass transport from bulk solution to a surface. The region of zero flow, $v=0$, is assumed to extend out a stagnant layer distance δ from the surface, beyond this the bulk solution moves at the average velocity of v_{BULK}. Transport from the bulk to the surface phase across zero flow region occurs predominantly *via* diffusion. (B) Ratio of steady-state stagnant flow region solute concentration to bulk solute concentration for different values of δ and different extents of initial adsorption rate and concentration of matrix adsorption sites, represented as a combined parameter $k_1(C_x)_{tot}$. The value of δ has been estimated on the basis of the 5% approximation discussed in the text. The value of $(C_x)_{tot}$ is calculated on the basis of the volume of the stagnant flow region, *i.e.* $(C_x)_{tot}$ decreases with increasing δ. (C) Typical differential rate plots for a system displaying Langmuir adsorption kinetics, which is highly influenced by mass transfer effects [dotted line: simulated using eqs. (4.9) and (4.14a)]. Differential rate plot for adsorption profile with the identical reaction kinetics but without mass transfer effects (solid line). The mass transfer limited data only approaches that of the Langmuir case at near maximal saturation of the adsorption matrix sites.

ıe stagnant point flow and the
›file of a fluid flowing over a
mit of contact with the surface
ınt layer may be considered as
surface. A neighboring similar-
the bulk, is considered to move

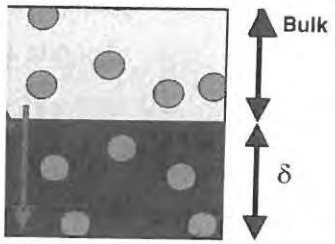

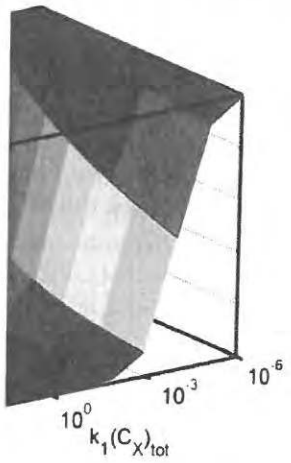

scribing mass transport from bulk
ro flow, $v = 0$, is assumed to extend
the surface, beyond this the bulk
of v_{BULK}. Transport from the bulk
v region occurs predominantly *via*
agnant flow region solute concen-
ır different values of δ and different
concentration of matrix adsorption
meter $k_1(C_x)_{tot}$. The value of δ has
ıpproximation discussed in the text.
basis of the volume of the stagnant
ncreasing δ. (C) Typical differential
gmuir adsorption kinetics, which is
ts [dotted line: simulated using eqs.
ot for adsorption profile with the
t mass transfer effects (solid line).
›roaches that of the Langmuir case
›rption matrix sites.

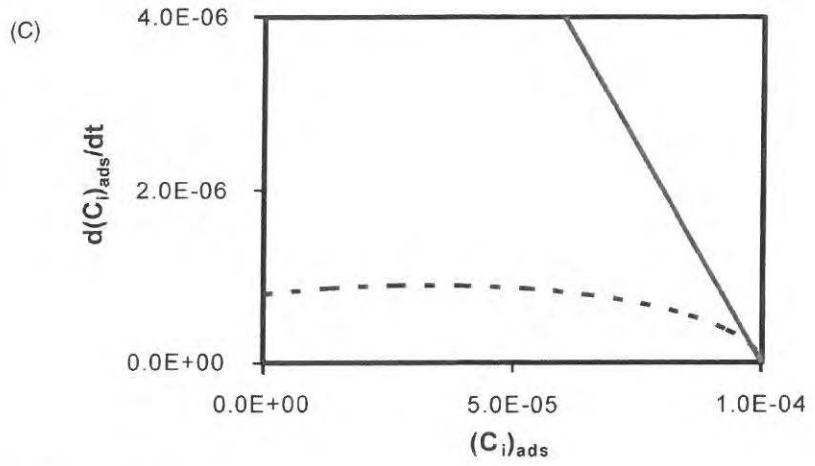

Figure 4.6 Continued

with a common averaged velocity, v_{BULK}. For relatively fast flow rates, transfer of solute from one region to another in the bulk will occur primarily by convection, allowing for the assumption of a single homogeneous compartment having a solute concentration designated C_{BULK} that is determined solely by the flow rate. Due to the assumed zero flow in the stagnant layer region close to the surface, transfer of solute from the bulk solution to the adsorptive surface over the distance δ will occur predominantly by diffusion. For such a simplified system the rate of solute transfer into the stagnant layer and the subsequent degree[16] of mass transfer limitation for an adsorption reaction (for a given receptor density, concentration of solute and intrinsic reaction kinetics) can be estimated *via* eq. (4.14).

$$\frac{d\{C_i\}}{dt} \approx \frac{D_i}{\delta^2}[C_{BULK} - \{C_i\}] - k_1'\{C_i\} \tag{4.14a}$$

$$\frac{\{C_i\}}{C_{BULK}} \approx \frac{D_i/\delta^2}{(D_i/\delta^2) + k_1'} \tag{4.14b}$$

Values of δ for different flow configurations and magnitudes of the stirring/flow rate have been calculated [28]; typical values[17] for current biosensor devices are of the order of micrometers [28,36]. In general, the parameter δ representing the thickness of the stagnant layer will become smaller upon

[16] Upper limit calculated by assuming irreversible reaction, *i.e.* $k_2 = 0\,s^{-1}$ and assuming steady-state $d\{C_i\}/dt = 0$. The assumption of $k_2 = 0$ is equivalent to the case of initial adsorption rate and hence mass transfer limitations will be at their greatest during initial adsorption rates.

[17] For solutes with diffusion coefficients of the magnitude of moderately sized globular proteins ($D \approx 1 \times 10^{-10}\,m^2\,s^{-1}$).

increasing the rate of flow.[18] Using eq. (4.14b), we have estimated the effect for the initial adsorption rate for various receptor densities and intrinsic kinetics of the adsorbing system in Figure 4.6a and the results are shown in Figure 4.6b. As can be noted, mass transfer limitations will be greatest for an adsorbing system (solute plus matrix site) having intrinsically rapid adsorption kinetics under experimental conditions where the adsorptive surface comprises a highly concentrated array of matrix sites and the fluid flow/stirring rate and the solute's diffusion coefficient are both of small magnitude. Such considerations have led to the general recommendation that optical biosensor experiments be conducted under conditions of low matrix concentration and high flow/stirring rates [42–45]. As illustrated in Figure 4.6c, mass transfer-limited adsorption data can be readily identified by the appearance of a downward curvature in plots of the adsorption rate *versus* the concentration of adsorbate [46]. In experimental studies of adsorption, the best approach is the elimination of any mass transfer effects by good experimental design. When this is technically not possible, a number of approximate strategies based on the two-state model described in eqs. (4.6) and (4.9) have been developed [33,37,38]. More will be said about the practical aspects of this extension to the standard analysis in Chapters 9 and 10. Now, however, having addressed the basics of the mass transfer process in optical biosensor experimentation, we turn our attention to the reaction component of the adsorption event.

4.2.2 Adsorption Mechanisms

In this section we formalize the discussion of adsorption mechanisms by deconstructing the subject into smaller component pieces.[19] We then use these building blocks to describe a wide range of adsorption behavior. By doing this we hope both to increase awareness of the pool of candidate models available for initial consideration and to educate the reader as to the richness in variety of adsorption behavior that is not confined to just the standard 1:1 binding model or variants thereof. In eq. (4.4) we have essentially pictured the adsorption reaction as the partition of a single solute for which the association rate function k_1' is sensitive to the concentration of adsorbate in a manner determined by the true

[18] One estimate of the magnitude of δ is on the basis of a 5% approximation, *i.e.* the value of δ at which the rate of solute transport into the stagnant region is less than 5% of the rate at which solute would enter *via* diffusion, *i.e.* $\delta \approx 0.05D_i/v(\delta)$. More detailed approaches to estimate δ or a δ-like parameter can be found in refs. [35,36] for cuvette systems and [40–41] for flow systems.

[19] Standard practice in the selection of a mechanistic model to describe experimental kinetic and equilibrium adsorption data involves selection of a number of likely candidate models followed by non-linear regression to find the model that best fits the data in a statistically relevant manner. There are a number of different strategies for performing such non-linear regression analysis of the data. Depending on the mathematical sophistication of the experimenter, this may be done using user-written software or user-defined models in a non-linear regression software package. Alternatively, a number of semi-"black box" routines are provided by the instrument manufacturers or interested third parties. A good starting point for information on the subject of modeling data by non-linear regression analysis can be found in ref. [47]. Discussion of the relative benefits of different fitting strategies is outside the scope of this chapter.

have estimated the effect for
ities and intrinsic kinetics of
ts are shown in Figure 4.6b.
e greatest for an adsorbing
ly rapid adsorption kinetics
e surface comprises a highly
flow/stirring rate and the
nitude. Such considerations
al biosensor experiments be
ation and high flow/stirring
transfer-limited adsorption
of a downward curvature in
ation of adsorbate [46]. In
ich is the elimination of any
When this is technically not
ed on the two-state model
ed [33,37,38]. More will be
to the standard analysis in
ssed the basics of the mass
on, we turn our attention to

tion mechanisms by decon-
[9] We then use these building
vior. By doing this we hope
models available for initial
ness in variety of adsorption
l binding model or variants
adsorption reaction as the
rate function k_1' is sensitive
determined by the true

proximation, *i.e.* the value of δ at
ess than 5% of the rate at which
iled approaches to estimate δ or a
ns and [40–41] for flow systems.
describe experimental kinetic and
cely candidate models followed by
in a statistically relevant manner.
on-linear regression analysis of the
erimenter, this may be done using
gression software package. Alter-
the instrument manufacturers or
n the subject of modeling data by
ussion of the relative benefits of

second-order adsorption association rate constant, k_1, the starting (hypothetical[20]) total concentration of matrix sites, $(C_x)_{tot}$, and the surface function, $f(\phi)$, describing the concentration of available sites for a given extent of surface occupation. By considering the process in this fashion we may neatly delineate our discussion of adsorption mechanisms into a number of separate sections. In the first section we will concern ourselves with general models of idealized partition occurring at a constant concentration of matrix sites [*i.e.* where $f(\phi)$ equals 1 and therefore k_1' equals $k_1(C_x)_{tot}$]. In the second section we will focus on how competition might affect the partition process of the single solute. In the third section we will describe how the surface function changes with different extents of surface occupation for different modes of adsorption.

4.2.2.1 Idealized Partition Processes

In chemistry, partition refers to the distribution of a solute between two immiscible liquid phases at infinitely dilute concentrations of the partitioning solute. In adsorption experiments, a similar situation is achieved when the solute is dilute and the adsorbate concentration is exceedingly low, thereby allowing us to equate $f(\phi)(C_x)_{tot}$ with $(C_x)_{tot}$. By examining the kinetics associated with this low-concentration region we may successfully divorce our analysis of adsorption from complications associated with any changes associated with the surface function. A single molecular adsorption event may occur as a mechanistically concerted adsorption event, observed to be occurring in a single elementary step [eq. (4.15)].[21]

$$\{C_1\} \underset{k_2}{\overset{k_1'}{\rightleftharpoons}} (C_1)_{ads} \tag{4.15}$$

Alternatively, a single molecular adsorption event may occur as a mechanistically stepwise process, whereby different parts of the adsorption process occur in a sequential manner with each event itself being defined by a unique characteristic time scale. Although potentially an indefinite number of intermediate forms of adsorbate may exist, *e.g.* $(C_{1a})_{ads}$, $(C_{1b})_{ads}$, ..., we express the general concept in a limited two-state model [eq. (4.16)].

$$\{C_1\} \underset{k_2}{\overset{k_1'}{\rightleftharpoons}} (C_{1a})_{ads} \underset{k_4}{\overset{F}{\rightleftharpoons}} (C_{1b})_{ads} \tag{4.16}$$

The rate of interconversion between $(C_{1a})_{ads}$ and $(C_{1b})_{ads}$ is respectively governed by forward and reverse rate constants F and k_4 (units of s^{-1}). If the forward rate of conversion is independent of the local concentration of matrix sites, F takes on a constant value of a simple first-order rate constant. If,

[20] By hypothetical we mean that the total concentration of adsorbate at maximal saturation may differ from the total starting concentration of matrix sites if an adsorbate molecule covers multiple potential binding sites.

[21] From here on we will make specific reference to the solute type, *i.e.* in this case we refer to the intimate concentration of solute of type 1 given by $\{C_1\}$.

however, the rate of interconversion is dependent on the local concentration of matrix sites, F represents a rate function composed, in the simplest case, of a second order rate constant k_3 (units of $1\,mol^{-1}\,s^{-1}$), the total concentration of matrix sites, $(C_x)_{tot}$ (and a stepwise specific surface function, $f_3(\phi_{1a}, \phi_{1b})$ that describes the fractional availability of nearby matrix sites and is dependent on the concentration of both types of adsorbed species.) The rate equation [describing the formation of adsorbate for a mechanistically concerted reaction denoted by eq. (4.15)] was given in eqs. (4.7)–(4.9) and is shown in Figure 4.7a.

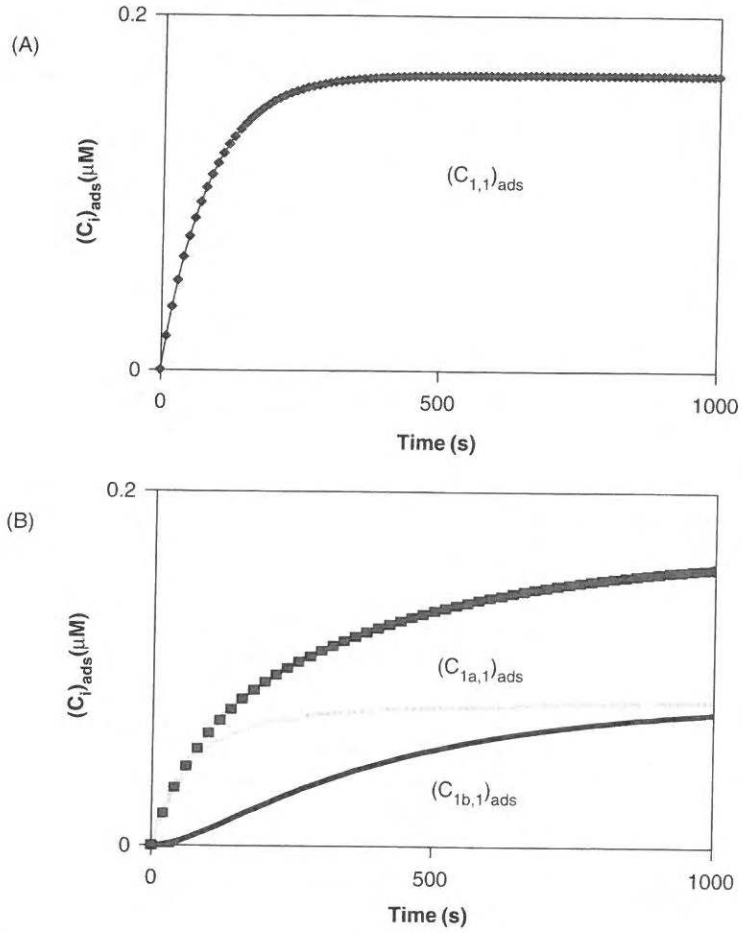

Figure 4.7 Adsorbate concentration *vs.* time in different partition processes. (A) Mechanistically concerted homogeneous partition (single class of solute and matrix site resulting in formation of single class of adsorbate $(C_{1,1})_{ads}$. (B) Mechanistically stepwise homogeneous isomerization (single class of solute and matrix site, adsorbate formation proceeds by way of a two-step reaction resulting in formation of two classes of adsorbate $(C_{1a,1})_{ads}$ and $(C_{1b,1})_{ads}$.

dent on the local concentration of
nposed, in the simplest case, of a
$^{-1}$ s^{-1}), the total concentration of
surface function, $f_3(\phi_{1a}, \phi_{1b})$ that
matrix sites and is dependent on
ped species.) The rate equation
nechanistically concerted reaction
(4.9) and is shown in Figure 4.7a.

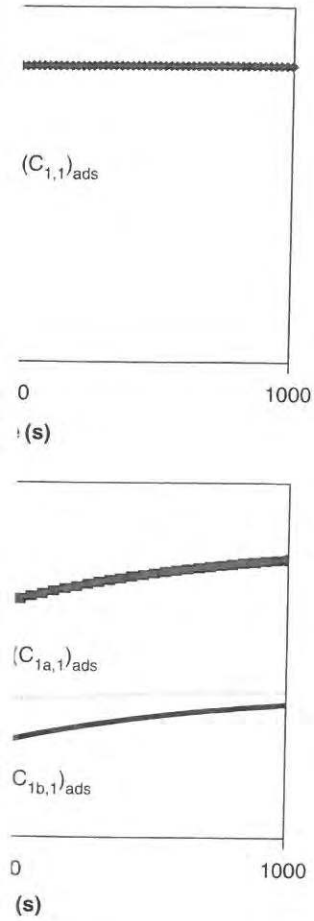

fferent partition processes. (A) Mech-
tition (single class of solute and matrix
ass of adsorbate $(C_{1,1})_{ads}$. (B) Mecha-
nerization (single class of solute and
ceeds by way of a two-step reaction
f adsorbate $(C_{1a,1})_{ads}$ and $(C_{1b,1})_{ads}$.

For a stepwise reaction, the rate of formation of the different classes of adsorbate[22] is given by eq. (4.17) (Figure 4.7b).

$$\frac{d(C_{1a})_{ads}}{dt} = k_1'\{C_1\} - k_2(C_{1a})_{ads} - F(C_{1a})_{ads} + k_4(C_{1b})_{ads} \tag{4.17a}$$

$$\frac{d(C_{1b})_{ads}}{dt} = F(C_{1a})_{ads} - k_4(C_{1b})_{ads} \tag{4.17b}$$

Assuming that the system is reversible, the most typical diagnostic for identifying adsorbate isomerization[23] is from analysis of a dissociation phase adsorption experiment [48]. Depending on the relative extents of occupation of the intermediate states, a bimodal signature of the rate plot of $d(C_1)_{ads}/dt$ *vs.* $(C_1)_{ads}$ will be apparent. Another diagnostic sign of adsorbate isomerization will be an apparent incompatibility between the dissociation rate calculated from analysis of the association phase and that calculated from the dissociation phase [48]. Examples of such isomerizing systems have been encountered in experimental studies of multivalent solutes; examples include antibody binding studies [49] and studies of multimeric proteins [50]. A detailed treatise of the theory can be found in ref. [51].

4.2.2.2 *Effect of Competing Reactions*

Depending on the nature of the experimental system (*i.e.* the solute, the adsorptive surface and the solvent conditions), there may exist a degree of heterogeneity in the effective strength of the interaction. This apparent heterogeneity may result from heterogeneity of the solute or heterogeneity of the matrix adsorption sites. Whatever the cause, analysis of heterogeneous binding data will result in an apparent distribution of rate constants whose influence will be felt according to the relative concentrations of the different types of solute and matrix adsorption sites. For the case where heterogeneity exists in the solute alone, such that a number p of different intimate solute types $[\{C_1\}, \ldots, \{C_p\}]$ exist, the observed rate of adsorption is given by the summation shown in eq. (4.18a). For the case where heterogeneity is caused by a certain number, q, of different types of matrix sites $[(C_x)_{tot(1)}, \ldots, (C_x)_{tot(q)}]$, the corresponding summation describing the rate of formation is that shown by eq. (4.18b). For the case where both the solute and the matrix site show heterogeneity, the double summation in eq. (4.18c) is required for an adequate description of the rate of adsorption.[24]

$$\sum_{j=1}^{j=p}\left[\frac{d(C_{j,1})_{ads}}{dt} = k'_{1(j,1)}\{C_j\} - k_{2(j,1)}(C_{j,1})_{ads}\right] \tag{4.18a}$$

[22] Again here limited to two for convenience.
[23] Another potential case of adsorbate isomerization is due to reaction of the adsorbate with other adsorbate molecules. This situation will be dealt with in the section on adsorbate clustering.
[24] The heterogeneity reaction can be extended to include conformational change.

$$\sum_{k=1}^{k=q}\left[\frac{\mathrm{d}(C_{1,k})_{\mathrm{ads}}}{\mathrm{d}t} = k'_{1(1,k)}\{C_1\} - k_{2(1,k)}(C_{1,k})_{\mathrm{ads}}\right] \tag{4.18b}$$

$$\sum_{j=1}^{j=p}\sum_{k=1}^{k=q}\left[\frac{\mathrm{d}(C_{j,k})_{\mathrm{ads}}}{\mathrm{d}t} = k'_{1(j,k)}\{C_j\} - k_{2(j,k)}(C_{j,k})_{\mathrm{ads}}\right] \tag{4.18c}$$

In the above formulation, the subscripted rate function, $k'_{1(j,\,k)}$ and rate constant $k_{2(j,\,k)}$ refer to the operative rate parameters for interaction between solute of type j and matrix site of type k to produce an adsorbate $(C_{j,\,k})_{\mathrm{ads}}$. Svitel *et al.* [52] have examined techniques for identifying and quantifying such heterogeneity in biosensor data for interactions obeying simple 1:1 binding models. Phenomenological descriptions of heterogeneity such as those described by eqs. (4.18a–c) also encompass competition reactions (Figure 4.8). One well-known example of a biological competition reaction is that discovered by Vroman *et al.* [53], in which the heterogeneous proteins of blood plasma were found to adsorb on glass with different characteristic time scales and binding affinities.

4.2.2.3 Surface Functions for Different Modes of Adsorption

For a surface denuded of adsorbate, all potential matrix sites are available for adsorption, making the surface function equal to 1. However, upon adsorption of solute the fraction of available matrix sites will change in a manner dictated by the way in which adsorbate molecules affect the likelihood of subsequent adsorption events. The mathematical form of this dependence is known as the surface function [54–59] and its exact nature will define the kinetic and equilibrium adsorption isotherms [60], *i.e.* the dependence of the rate and equilibrium extent of adsorption on the concentration of intimate solute for a given adsorbate concentration (and set solution composition and temperature). Here we make use of simple geometric approximations to describe the physical nature of the solute and adsorptive surface and treat attractive and repulsive behavior through simple interaction potentials such as hard particle approximations or square well potentials (mesoscopic models). These mesoscopic models are used here to describe the surface function for various adsorptive behaviors. Such approaches are especially suited to the aims of this chapter, in which kinetic models are used to comment on the phenomenon of adsorption from the viewpoint of a measurement device that provides a single observable experimental parameter related to the total concentration of all species adsorbed at the interfacial layer. With this proviso, we begin our description of surface functions by first more carefully defining the meaning of the quantity ϕ.

For the simple case of a spherical adsorbing solute, the surface function is expressed in terms of the quantity ϕ_i, which expresses the ratio of the concentration of adsorbate to the total concentration of matrix sites multiplied by n_i, a

$_{2(1,k)}(C_{1,k})_{ads}\Big]$ (4.18b)

$k_{2(j,k)}(C_{j,k})_{ads}\Big]$ (4.18c)

te function, $k'_{1(j,\,k)}$ and rate
ıeters for interaction between
)duce an adsorbate $(C_{j,\,k})_{ads}$.
ntifying and quantifying such
; obeying simple 1:1 binding
:rogeneity such as those de-
:tition reactions (Figure 4.8).
ion reaction is that discovered
)us proteins of blood plasma
:haracteristic time scales and

Modes of Adsorption

matrix sites are available for
1. However, upon adsorption
l change in a manner dictated
the likelihood of subsequent
s dependence is known as the
l define the kinetic and equi-
dence of the rate and equilib-
of intimate solute for a given
sition and temperature). Here
ons to describe the physical
treat attractive and repulsive
uch as hard particle approxi-
models). These mesoscopic
ıction for various adsorptive
l to the aims of this chapter,
ıe phenomenon of adsorption
ıat provides a single observ-
l concentration of all species
)viso, we begin our descrip-
defining the meaning of the

;olute, the surface function is
'esses the ratio of the concen-
matrix sites multiplied by n_i, a

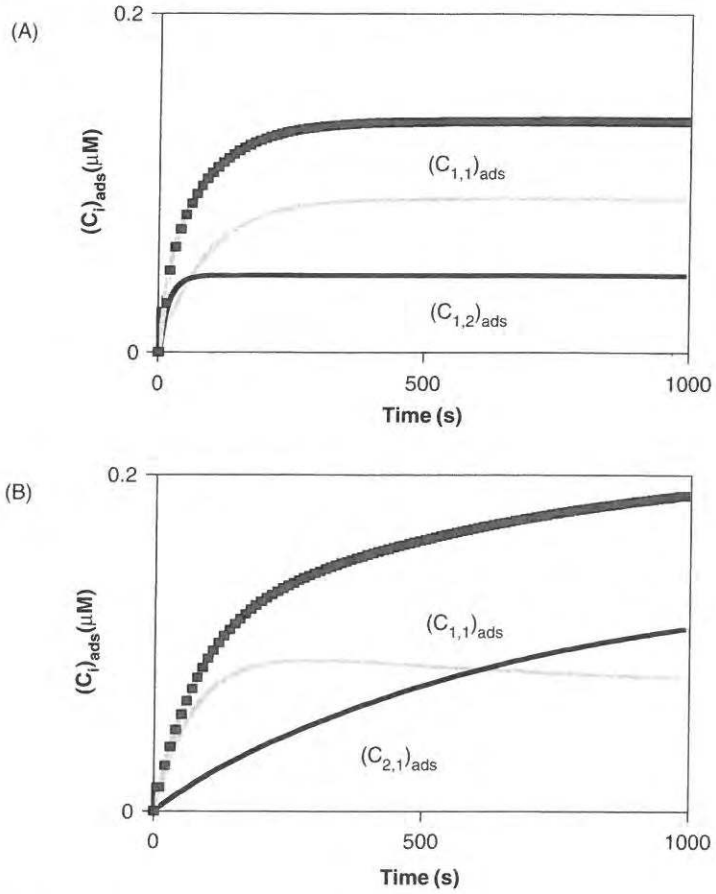

Figure 4.8 Adsorbate concentration *versus* time for different competition processes. (A) Mechanistically concerted heterogeneous partition [one class of solute and two classes of matrix site resulting in formation of two classes of adsorbate $(C_{1,1})_{ads}$ and $(C_{1,2})_{ads}$]. (B) Mechanistically concerted heterogeneous partition [two classes of solute and one class of matrix site resulting in formation of two classes of adsorbate $(C_{1,1})_{ads}$ and $(C_{2,1})_{ads}$].

term representing the average number of matrix sites physically covered by adsorbate of type i [eq. (4.19)].[25]

$$\phi_i = \frac{n_i(C_i)_{ads}}{(C_x)_{tot}} \approx \frac{(\rho_i *)_{ads}\pi r_i^2}{A_{tot}} \tag{4.19}$$

At very low densities of matrix sites, such that adsorption at one site does not influence adsorption at another, $n_i = 1$. At high matrix densities relative to the size of the solute (see Figure 4.1), the matrix will approach the continuum limit

[25] The surface function will be a function of the relative orientation for an asymmetric adsorbate but we do not treat that complication here.

(approximation shown in brackets). In this case, one may estimate the value of n on the basis of geometric arguments alone. For planar adsorptive surfaces characterized by an area density ρ_x^* of matrix sites (molecules m^{-2}) or three-dimensional adsorptive surfaces characterized by a volume density of matrix sites ρ_x (molecules m^{-3}), we may approximate n_i from knowledge of the physical area and volume covered by the adsorbate yielding eqs. (4.20a) and (4.20b), respectively.

$$n_i \rightarrow \rho_x^* \pi r_i^2 \quad \text{at high densities for 2D surfaces} \tag{4.20a}$$

$$n_i \rightarrow \rho_x (4/3) \pi r_i^3 \quad \text{at high densities for 3D surfaces} \tag{4.20b}$$

In discussing surface functions, we recognize that adsorption reactions can be categorized into two general types [60], those capable of being saturated (*i.e.* a fixed number of adsorption sites) and those incapable of being saturated (non-fixed number of adsorption sites, usually corresponding to multilayer formation) (Figure 4.9). In optical biosensor experimentation involving biological macromolecules, both types of adsorption are encountered [61,62] so we discuss the general characteristics of each in turn.

Surface Phases Capable of Being Saturated. In the case of adsorptive surfaces that are capable of being saturated, the simplest form that the surface function can take is that suggested by Langmuir [63], whereby adsorption to any particular matrix site is independent of all others and each binding event decreases the total number of matrix sites by one (such that $n_i = 1$). For a single class of solute adsorbing to a single class of matrix site, we have [eq. (4.21)].

$$f_{1(1,1)}(\phi_{1,1}) = 1 - \phi_{1,1} \tag{4.21}$$

Provided that the necessary conditions concerning independence and capacity for saturation described above are met, the Langmuir model may be extended to describe the case of a heterogeneous solute or heterogeneous matrix site. For the most general case of both heterogeneous solute and matrix [Eq. (4.18c)], a separate surface function for each of the k types of matrix sites, $f_{1(j,k)}$, can be written as eq. (4.22), again within the remit of the Langmuir requirements.

$$f_{1(j,k)}\left(\phi_{1,k}, \ldots, \phi_{p,k}\right) = 1 - \sum_{j=1}^{p} \phi_{j,k} \tag{4.22}$$

If the matrix sites are densely packed relative to the matrix site spacing, the adsorption of a solute molecule will influence the potential for adsorption of other solute molecules in the vicinity. This influence may be repulsive, in which case the surface function will decrease more sharply with increasing adsorbate concentration than a corresponding hypothetical Langmuir isotherm[26] [60].

[26] By corresponding hypothetical Langmuir isotherm we mean one defined by a surface function in which the total concentration of matrix sites $(C_x)_{tot}$ is not the true concentration of matrix sites but that corresponding to the maximal adsorbate concentration $(C_i)_{ads}$.

ase, one may estimate the value
alone. For planar adsorptive
of matrix sites (molecules m^{-2})
racterized by a volume density
approximate n_i from knowledge
e adsorbate yielding eqs. (4.20a)

s for 2D surfaces (4.20a)

or 3D surfaces (4.20b)

e that adsorption reactions can
e capable of being saturated (*i.e.*
se incapable of being saturated
lly corresponding to multilayer
experimentation involving bio-
on are encountered [61,62] so we
rn.

n the case of adsorptive surfaces
t form that the surface function
3], whereby adsorption to any
others and each binding event
ie (such that $n_i = 1$). For a single
atrix site, we have [eq. (4.21)].

$\phi_{1,1}$ (4.21)

ning independence and capacity
gmuir model may be extended to
terogeneous matrix site. For the
ite and matrix [Eq. (4.18c)], a
es of matrix sites, $f_{1(j,k)}$, can be
the Langmuir requirements.

$1 - \sum_{j=1}^{p} \phi_{j,k}$ (4.22)

e to the matrix site spacing, the
the potential for adsorption of
ence may be repulsive, in which
arply with increasing adsorbate
ical Langmuir isotherm[26] [60].

an one defined by a surface function in
he true concentration of matrix sites but
on $(C_i)_{ads}$.

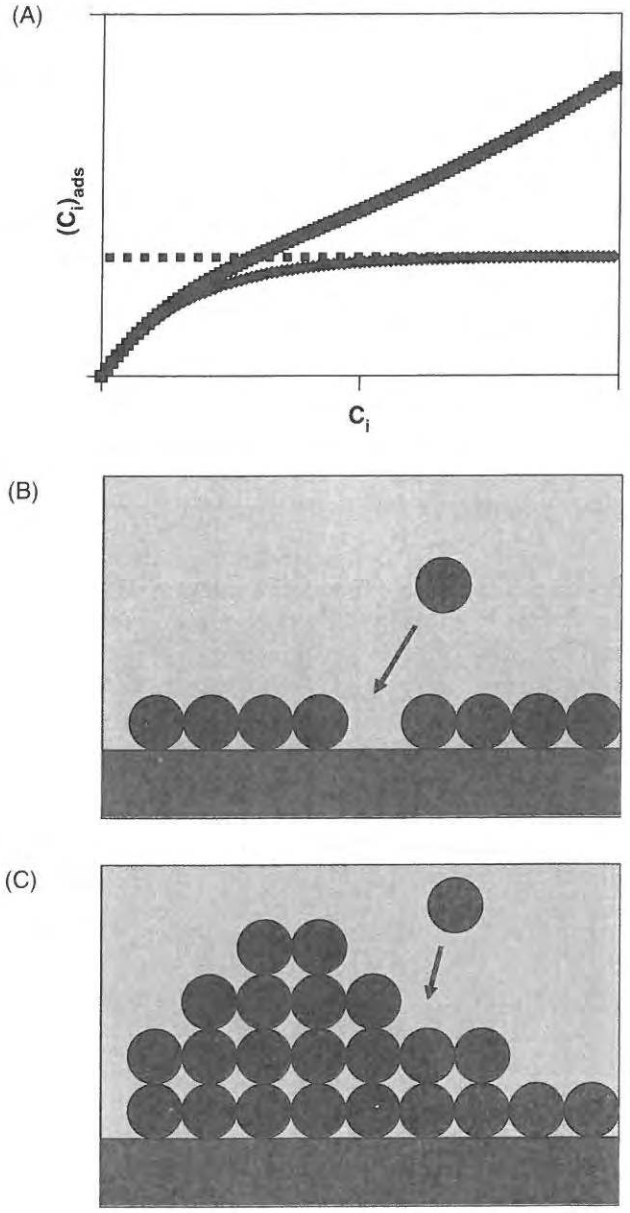

Figure 4.9 (A) Illustration of two general cases of adsorption behavior. Lower trace: saturation due to a fixed number of sites and monolayer formation (saturation implies that no further adsorption will take place despite increasing the concentration of solute). Upper trace: the type of adsorption that cannot be saturated due to multilayer adsorption. The dotted line represents monolayer coverage. (B) Diagram showing apparent monolayer coverage for saturated adsorption. (C) Diagram showing apparent multilayer formation for adsorption not capable of being saturated.

Alternatively, if the influence is attractive, the extent of decrease in the surface function *versus* the Langmuir case will lessen. At very high extents of attraction the surface function may even mimic that associated with the Langmuir case [64].

The simplest manner of incorporating symmetrical repulsive interactions into the surface function is to approximate the repulsive interaction by an equivalent interaction of hard circles for planar (two-dimensional) surface phases and hard spheres for three-dimensional surface phases [54,57] (Figure 4.10). Such approaches usually take one of two general forms, depending on the extent of the reversibility of the adsorption event or the degree of mobility of the surface phase. For highly mobile surfaces and/or rapidly dissociating systems, equilibrium fluid models based on scaled particle theory (SPT) expansions [65,66] are particularly useful for describing the surface function. For the case of adsorption of a single class of solute to a 2D continuum of a single class of matrix sites we have eq. (4.23).

$$f_{1(1,1)}(\phi_1) = \exp\left\{-\left[-\ln(1-\phi_1) + \frac{2\phi_1}{1-\phi_1} + \frac{\phi_1}{(1-\phi_1)^2}\right]\right\} \tag{4.23}$$

The SPT models can easily accommodate a range of different size adsorbates existing on the surface by making the surface function for a given elementary step and a certain class j of solute, a function of the different extents of fractional coverage of all the different adsorbate types on a single class of surface matrix sites $\phi_{1,1}, \phi_{2,1}, \ldots, \phi_{n,1}$, *e.g.* $f_{1(j,1)}(\phi_{1,1}, \phi_{2,1}, \ldots, \phi_{n,1})$. For a range of different sized adsorbate molecules characterized by radii r_i and surface densities ρ_i^* (for a two-dimensional adsorptive surface), the surface function describing the probability of finding a free matrix site is approximated by eq. (4.24), for convenience expressed in radii of adsorbate on a near continuum of matrix sites on the surface.

$$f_{1,(j,1)}(r_1, \ldots, r_n) = \exp\left\{-\left(-\ln\left[1-\pi\sum\left(\rho_i^* R_i^2\right)\right] + \left[\frac{2\pi\left(\sum \rho_i^* R_i\right)}{1-\pi\sum \rho_i^* R_i^2}\right] R_j + \left[\frac{\pi\sum \rho_i^*}{1-\pi\sum \rho_i^* R_i^2} + \frac{\pi^2\left(\sum \rho_i^* R_i\right)^2}{\left(1-\pi\sum \rho_i^* R_i^2\right)^2}\right] R_j^2\right)\right\} \tag{4.24}$$

For irreversible adsorption reactions ($k_2 = 0\,\mathrm{s}^{-1}$), which occur on an adsorptive surface with matrix sites fixed in position (termed immobile), the form of the surface function will be more appropriately described by a modeling approach based on the phenomenon of random sequential adsorption (RSA) [67,68]. At high levels of surface coverage, the surface distribution of adsorbate will be, on average, less efficiently placed and this more "selfish packing" will result in a reduced maximal extent of adsorption, $\phi_{\max}$. For monolayer adsorption of one class of solute to a planar continuum surface, the maximal extent of surface coverage for a reversible (or alternatively highly mobile surface) adsorption reaction is $\phi_{\max} = 0.906$, and for an irreversible adsorption

tent of decrease in the surface very high extents of attraction ed with the Langmuir case [64]. rical repulsive interactions into lsive interaction by an equiv- -dimensional) surface phases phases [54,57] (Figure 4.10). eral forms, depending on the it or the degree of mobility of s and/or rapidly dissociating d particle theory (SPT) expan- the surface function. For the 2D continuum of a single class

$$\left.\frac{1}{\phi_1}+\frac{\phi_1}{(1-\phi_1)^2}\right]\Bigg\} \qquad (4.23)$$

ge of different size adsorbates nction for a given elementary n of the different extents of te types on a single class of $)(\phi_{1,1}, \phi_{2,1}, \ldots, \phi_{n,1})$. For a haracterized by radii r_i and sorptive surface), the surface ee matrix site is approximated dii of adsorbate on a near

$$\left.{}_i^* R_i^2)\right] + \left[\frac{2\pi(\sum \rho_i^* R_i)}{1-\pi\sum \rho_i^* R_i^2}\right] R_j$$

$$\left.\frac{\sum \rho_i^* R_i)^2}{\sum \rho_i^* R_i^2)^2}\right] R_j^2\Bigg)\Bigg\}$$

(4.24)

$^{-1}$), which occur on an ads- (termed immobile), the form ely described by a modeling sequential adsorption (RSA) ace distribution of adsorbate s more "selfish packing" will tion, ϕ_{max}. For monolayer tinuum surface, the maximal alternatively highly mobile or an irreversible adsorption

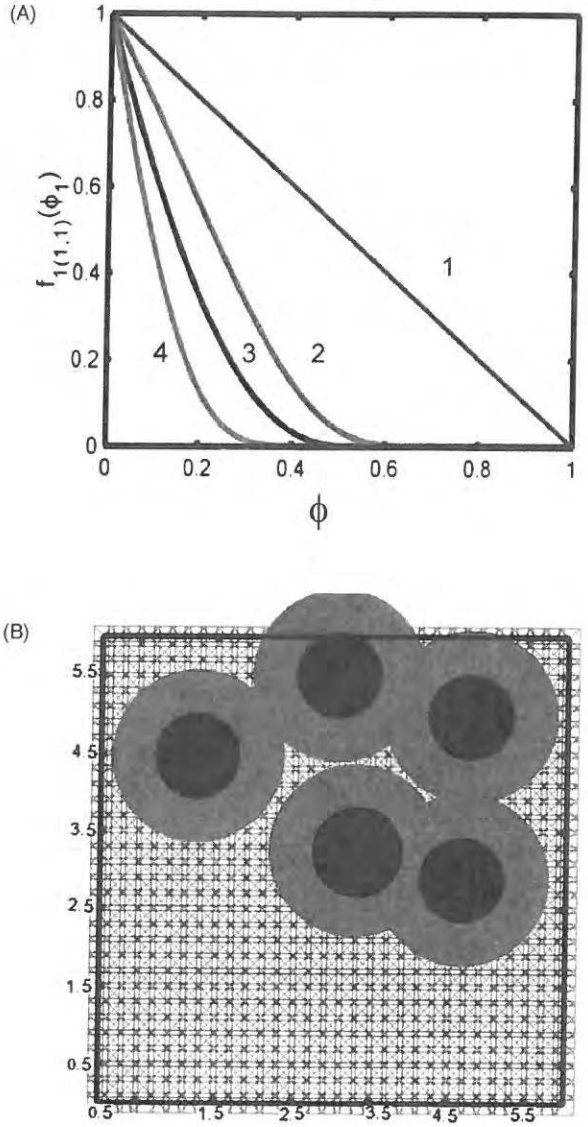

Figure 4.10 Adsorption behavior showing a saturation limit: repulsive adsorbate–adsorbate interactions. (A) Surface functions for adsorption of a single class of monomeric spherical solute to a single class of adsorptive surface sites *versus* fractional surface coverage for (1) Langmuir case [eq. (4.21)], (2) 2D – equilibrium fluid calculation [eq. (4.23)], (3) random sequential adsorption calculation [eq. (4.25)] and (4) 3D – equilibrium fluid calculation [eq. (4.26)]. (B) Illustration of the rapid decrease in the surface functions for the particle model based cases [lines 2–4 in (A)]. Suboptimal placement leads to a rapid decrease in the number of available sites. Here black circles represent adsorbate and red halos denote area excluded for subsequent solute adsorption.

reaction occurring on an immobile adsorptive surface the corresponding value of ϕ_{max} is 0.546 [54]. The surface function from such irreversible random sequential adsorption of a single class of solute to a planar surface has been calculated by Monte Carlo-based computer simulations [55]. A compact polynomial description of the results of such simulations is given by eq. (4.25).

$$f_{1,(1,1)}(\phi_1) = \frac{(1 - \{\phi_1/\phi_{max}\})^3}{1 - 0.812\{\phi_1/\phi_{max}\} + 0.2336\{\phi_1/\phi_{max}\}^2 + 0.0845\{\phi_1/\phi_{max}\}^3} \tag{4.25}$$

At high extents of surface coverage, somewhere between the limits of irreversible adsorption to an immobile surface and reversible adsorption to a highly mobile phase, one may encounter kinetics reminiscent of a glassy state to ordered state phase transition [69]. In this regime the rate at which the surface function changes from the random sequential model to the equilibrium SPT model will be determined by the kinetics of reorganization of the surface phase dictated by the rate constants k_1 and k_2 and the adsorptive surface phase matrix site diffusion constants [70].

For a three-dimensional surface phase such as that presented by matrix sites existing on a carboxymethyldextran gel layer derivatized with specific matrix sites, the calculation/estimation of fractional site coverage and maximal extent of occupation is more difficult.[27] In the volume transcribed by the gel layer a significant volume fraction is already occupied by the gel itself [31]. Additionally, the fractional availability of matrix sites will in part be determined by mass transfer into the gel layer. As solute will enter the surface phase from the top, these surface sites will be preferentially occupied, possibly preventing access to matrix sites below [32]. A possible starting point for the calculation of approximate surface functions for a highly derivatized gel matrix has been suggested [71], which involves treating the gel layer as a 3D phase with evenly dispersed matrix sites. Using such an approach one may calculate[28] $f_1(\phi_1)$ for a single class of adsorbing solutes using the 3D version of the SPT equation [66] [eq. (4.26)].

$$f_{1(1,1)}(\phi_1) = \exp\left\{-\left(-\ln(1-\phi_1) + \left[\frac{7\phi_1}{(1-\phi_1)}\right] + \left[\frac{7.5\phi_1^2}{(1-\phi_1)^2}\right] + \left[\frac{3\phi_1^3}{(1-\phi_1)^3}\right]\right)\right\} \tag{4.26}$$

For the alternative case of attractive surface interactions resulting in preferential cluster formation, the surface function will decrease less sharply than for the purely repulsive surface interaction case with increasing adsorbate

[27] For freely accessible insertion of spheres into an open volume, ϕ_{max} varies between 0.636 and 0.7405 for the equilibrium random and jamming close packing limit.

[28] Using eq. (4.20b) for the estimation of n_1 and neglecting the presence of the gel layer as a first approximation.

concentration and may even approach the behavior defined by the surface function for the Langmuir isotherm [64]. For a highly mobile/reversible surface, clustering may occur *via* a post-adsorption interaction in a stepwise reaction event (Figure 4.11a) and may be viewed as a type of isomerization reaction as derived in eq. (4.17). Alternatively, clustering of adsorbate may occur as part of the elementary process of adsorption (Figure 4.11b) [72]. With regard to the first mode of cluster formation (monomer adsorption followed by cluster growth), we present a cluster isomerization/growth model based on monomeric adsorbate addition and monomeric adsorbate loss in eq. (4.27) on a single class of matrix sites. In this model, an adsorbate cluster containing i monomers is specified by $(C_1)_{ads[i]}$ and the intrinsic association and dissociation rate constants for clusters of size i on the surface as $k_{3[i]}$ and $k_{4[i]}$, respectively. By varying the rate constants for formation of a cluster of i monomers, $k_{3[i]}$ and dissociation of an adsorbate from a cluster of i monomers into monomeric adsorbate and a cluster of size $(i - 1)$ monomers, $k_{4[i]}$, between large and low values one can describe the widest possible range of behavior corresponding to a high mobility and low mobility surface phase, for the case where the attractive potential exerted

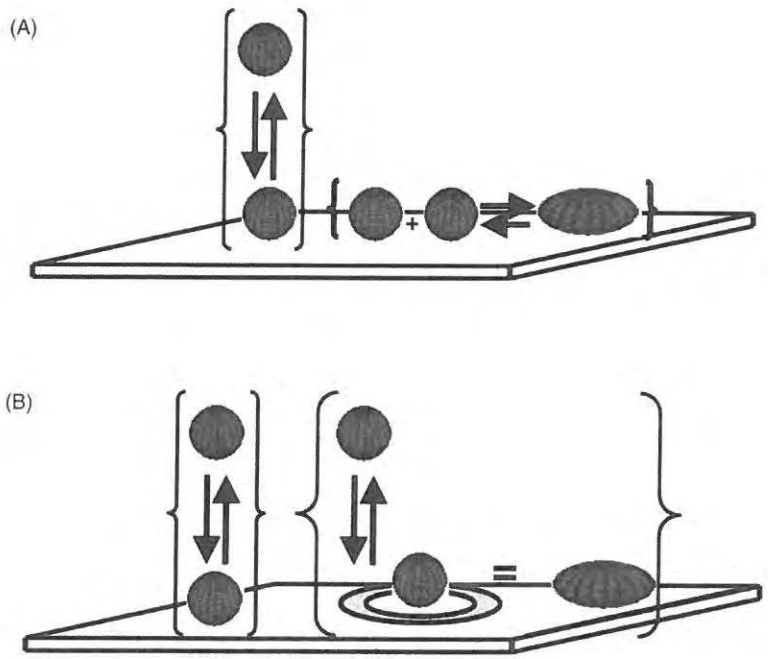

Figure 4.11 Adsorption behavior showing a saturation limit: attractive adsorbate–adsorbate interactions resulting in cluster formation happening as a result of (A) post-adsorption association due to surface mobility and (B) association occurring in concert with the adsorption event.

by the cluster does not increase the rate of solute adsorption but only effects the rate of adsorbate desorption.

$$\frac{d(C_1)_{ads[1]}}{dt} = k_1'\{C_1\} - k_2(C_1)_{ads[1]} + \left[\sum_{i=2}^{Z} -k_{3[i]}(C_1)_{ads[1]}(C_1)_{ads[i]} + k_{4[i]}(C_1)_{ads[i]}\right] \quad (4.27a)$$

$$\frac{d(C_1)_{ads[i]}}{dt} = k_{3[i]}(C_1)_{ads[1]}(C_1)_{ads[i-1]} - k_{4[i]}(C_1)_{ads[i]} - k_{3[i+1]}(C_1)_{ads[1]}(C_1)_{ads[i]} + k_{4[i+1]}(C_1)_{ads[i+1]} \text{ for } 2 \leq i < z \quad (4.27b)$$

$$\frac{d(C_1)_{ads[z]}}{dt} = k_{3[z]}(C_1)_{ads[1]}(C_1)_{ads[z-1]} - k_{4[z]}(C_1)_{ads[z]} \text{ for } i = z \quad (4.27c)$$

For cluster formation occurring in 2D, an initial approximation of the system can be made by modeling each cluster of i monomers as a circular aggregate of radius $r_i = r_1 i$, thus allowing the use of surface functions described for the 2D continuum surface phase [eq. (4.24)].[29]

Figure 4.12a describes the change in surface function for the situation when, on the time-scale of adsorption, clustering is rapid. In the alternative case, where cluster growth occurs contemporaneously with the adsorption event, we model cluster formation by defining an attractive potential that contributes a stabilizing energy, ΔE_c, to monomer adsorbed in an area surrounding an already adsorbed monomer or cluster. For simplicity, the stabilizing potential can be considered as a square well that projects a small distance d from the cluster perimeter and the distance of closest approach.[30] When comparing monomer adsorption to two equal areas of surface, one existing within the attractive well and the other outside it, the overall affinity of the monomer for the adsorptive surface is modified by a unitless factor K_C [eq. (4.28)].

$$K_C = \exp\left(\frac{-\Delta E_C}{RT}\right) \quad (4.28)$$

Equation (4.28) represents an equilibrium stabilization factor. However, for a kinetic model one needs to parse out the contributions into the individual forward and reverse rate constants. In principle, the stabilizing effect could be

[29] Note that in reality the cluster will be a chain of aggregated adsorbate having a shape that will display fractal-like characteristics. This fractal-like quality will have an effect on the adsorption kinetics. This topic is dealt with in Chapter 5.

[30] For reasons of stability of the solution of equations, we actually consider that the zone of attractive potential associated with adsorbate species lies between the distance of closest approach $(r_1 + r_i)$ and a smaller distance $(r_1 + r_i - d)$. Such an approximation will not significantly change the form of the effect upon the surface function. Additionally, this approximation will allow for the estimation of an approximate surface function for this clustering mode up to fairly high degrees of surface occupation (however, it will be less reliable as ϕ approaches its maximum value). The distance d should be chosen so that it is less than r_1.

adsorption but only effects

(4.27a)

$+ k_{4[i]}(C_1)_{ads[i]}\Big]$

(4.27b)

$_{ads[i+1]}$ for $2 \leq i < z$

$)_{ads[z]}$ for $i = z$ (4.27c)

itial approximation of the
i monomers as a circular
surface functions described

tion for the situation when,
id. In the alternative case,
th the adsorption event, we
potential that contributes a
n an area surrounding an
ty, the stabilizing potential
small distance d from the
roach.[30] When comparing
ce, one existing within the
ffinity of the monomer for
or K_C [eq. (4.28)].

(4.28)

zation factor. However, for
outions into the individual
e stabilizing effect could be

dsorbate having a shape that will
have an effect on the adsorption

tually consider that the zone of
n the distance of closest approach
ition will not significantly change
s approximation will allow for the
mode up to fairly high degrees of
oaches its maximum value). The

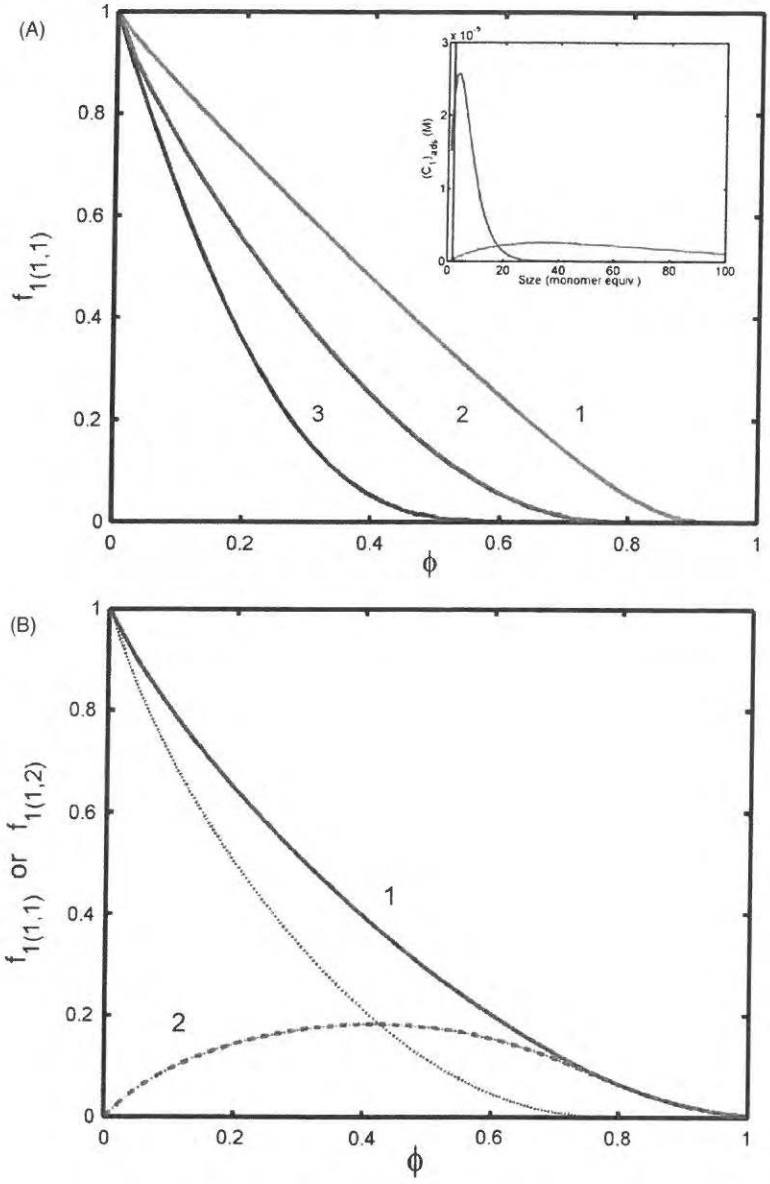

Figure 4.12 (A) Surface function for the post-adsorption cluster formation case as a function of the extent of cluster formation (line 1, $k_3/k_4 = 1$; line 2, $k_3/k_4 = 100$; line 3, $k_3/k_4 = 1000$). Inset describes the corresponding size distributions of adsorbate on surface for the three different values of k_3/k_4 – note that for the lowest value of k_3/k_4 the adsorbate exists exclusively as monomer. (B) Surface functions for the case of cluster formation occurring in concert with adsorption. Line 1 describes $f_{1(1,1)}$ and line 2 describes $f_{1(1,2)}$. The interaction distance was set at $d = 0.3r_1$. The additional line represents the calculation of the surface function for the reduced radius [see eq. (4.30a) and footnote 31].

housed either entirely in k_1 or entirely in k_2. For purposes of discussion the effect is divided equally by modifying the idealized adsorption partition rate constant of monomer to cluster by the factor $\sqrt{(K_C)}$ and the adsorption dissociation rate constant of monomer from a cluster by the factor $1/\sqrt{(K_C)}$. In this case, the intrinsic rate constants describing monomer adsorption to a region of surface within the attractive cluster potential are described by eq. (4.29). For an already occupied surface the attractive well around each adsorbate cluster effectively constitutes a different class of matrix sites to that existing outside the zone of attractive potential, similar to the heterogeneous case in eq. (4.18b), for which there are two classes of matrix site.

$$k_{1(1,2)} = k_{1(1,1)}\sqrt{K_C} \quad \text{and} \quad k_{2(1,2)} = \frac{k_{2(1,1)}}{\sqrt{K_C}} \tag{4.29}$$

For such a case we may estimate the surface function for the "first" class of sites (matrix alone) using eq. (4.24). The surface function for the "second" class of sites can be calculated as the difference between surface functions calculated on the basis of circular species of true radius and species of modified radius $r_i - d$ [see footnote 31 – eq. (4.30a)]. The surface function specifically associated with each cluster composed of i monomers, $f_{1(1,2)\{i\}}$, can be parsed out by multiplying eq. (4.30a) by the surface area of the potential region around the i-sized cluster and dividing by the total area associated with all regions of attractive potential [Eq. (4.30b)].

$$f_{1,(1,2)} \approx f_{1,(1,1)}[(r_1 - d), \ldots, (r_n - d)] - f_{1,(1,1)}(r_1, \ldots, r_n) \tag{4.30a}$$

$$f_{1,(1,2)[i]} = f_{1,(1,2)} \frac{(C_1)_{\text{ads}[i]}(r_i + r_1 - d)^2}{\sum_{k=1}^{z} (C_1)_{\text{ads}[k]}(r_k + r_1 - d)^2} \tag{4.30b}$$

By modeling each growing cluster as a circle that grows and shortens by either addition or loss of a monomer unit, the rate of formation of each cluster of k monomers can be expressed using eqs. (4.31a–c). Figure 4.12b describes the change in surface functions for this mode of adsorption with varying adsorbate levels.

$$\begin{aligned} \frac{\mathrm{d}(C_1)_{\text{ads}[1]}}{\mathrm{d}t} = {} & k'_{1(1,1)[1]}\{C_1\} - k_{2(1,1)[1]}(C_1)_{\text{ads}[1]} \\ & - k'_{1(1,2)[2]}\{C_1\} + k_{2(1,2)[2]}(C_2)_{\text{ads}[2]} \end{aligned} \tag{4.31a}$$

$$\begin{aligned} \frac{\mathrm{d}(C_1)_{\text{ads}[k]}}{\mathrm{d}t} = {} & k'_{1(1,2)[k]}\{C_1\} - k_{2(1,2)[k]}(C_1)_{\text{ads}[k]} \\ & - k'_{1(1,2)[k+1]}\{C_1\} + k_{2(1,2)[k+1]}(C_k)_{\text{ads}[k+1]} \end{aligned} \tag{4.31b}$$

$$\frac{\mathrm{d}(C_1)_{\text{ads}[z]}}{\mathrm{d}t} = k'_{1(1,2)[z]}\{C_1\} - k_{2(1,2)[z]}(C_1)_{\text{ads}[z]} \tag{4.31c}$$

r purposes of discussion the
ed adsorption partition rate
$\sqrt{(K_C)}$ and the adsorption
uster by the factor $1/\sqrt{(K_C)}$.
g monomer adsorption to a
potential are described by
attractive well around each
t class of matrix sites to that
similar to the heterogeneous
s of matrix site.

$$_{1,2)} = \frac{k_{2(1,1)}}{\sqrt{K_C}} \qquad (4.29)$$

nction for the "first" class of
nction for the "second" class
surface functions calculated
pecies of modified radius r_i –
nction specifically associated
$_{1,2)\{i\}}$, can be parsed out by
potential region around the
sociated with all regions of

$$_{(1,1)}(r_1, \ldots, r_n) \qquad (4.30a)$$

$$\frac{r_1 - d)^2}{+ r_1 - d)^2} \qquad (4.30b)$$

grows and shortens by either
rmation of each cluster of k
. Figure 4.12b describes the
ption with varying adsorbate

$$_1](C_1)_{\text{ads}[1]} \qquad (4.31a)$$
$$_{,2)[2]}(C_2)_{\text{ads}[2]}$$

$$_{\text{ds}[k]} \qquad (4.31b)$$
$$_1](C_k)_{\text{ads}[k+1]}$$

$$_{)[z]}(C_1)_{\text{ads}[z]} \qquad (4.31c)$$

Surface Phases Capable of Supporting Multilayer Growth. The treatment of multilayer growth is a complex problem which has received a number of reviews [73,74] and is important in many areas as diverse as semiconductor preparation [75], gas wetting phenomena [76] and bio-nanotechnology [77]. Here, the aim is to provide a basic introduction to the subject that goes beyond the usual cursory mention of the BET isotherm [78] by using simple models to outline some limiting case behaviors of the major types of multilayer adsorption growth (Figure 4.12). As it vastly decreases the complexity while still providing much chemical insight, we will restrict our kinetic description of multilayer growth that proceeds effectively irreversibly (*i.e.* $k_2 \rightarrow 0\,s^{-1}$).

If the fractional coverage and pertinent rate parameters applicable to the first and subsequent layers are additionally appended by the subscripts {L1}, {L2}, . . . , then a full kinetic description of the system can be made by solving one of the candidate surface functions for the primary adsorption layer $_{\{L1\}}$ and for each consecutive surface layer above layer one, {L2}, {L3}, . . . , *etc.* To aid our discussion of multilayer formation we will employ the formalism just described which pictures cluster formation as a form of heterogeneous adsorption. By varying the value of $k_{1(1,1)}$ and K_C [eq. (4.29)] for each adsorption layer, one can effectively describe many different modes of multilayer formation.

One of the simplest multilayer growth modes is that of the Frank–van der Merwe type, shown in Figure 4.13a [79]. This type of multilayer growth involves sequential deposition of one layer to top of the previous layer. This multilayer formation results from the fact that adsorption occurring in concert with cluster formation is highly favored over adsorption in the absence of cluster formation *e.g.* for an arbitrary layer i, $k_{1(1,2)\{Li\}} \gg k_{1(1,1)\{Li\}}$. In this limit, the overall vertical rate of growth of the multilayer will be much slower than its rate of lateral growth and adsorption of the new layer will generally occur after deposition in the underlying layer has achieved a significant coverage. In analogy with condensation or crystallization phenomena, one may liken the first adsorption event to each new layer as a nucleation event which is followed by a growth event (layer growth proceeding to coverage) [73]. As the layer becomes significantly covered, the chance of another nucleation event becomes greater and the process may begin again. If the horizontal and vertical adsorption rates are approximately equal [$k_{1(1,2)\{Li\}} \approx k_{1(1,1)\{Li\}}$] a different type of multilayer adsorption behavior, known as Volmer–Weber growth [80] or island growth, is observed (Figure 4.13b). In this case, adsorption mounds are formed separate from each other. Similar reasoning can be used to describe the phenomena of columnar multilayer growth shown in Figure 4.13c [81]. In this situation, the vertical adsorption rate far outweighs the lateral adsorption rate [$k_{1(1,2)\{Li\}} \ll k_{1(1,1)\{Li\}}$], leading to the growth of columns that may or may not be vertical, depending on the initial orientation of the first adsorbing molecules and/or the degree of surface roughness.

Although a complete description of the adsorption kinetics for multilayer growth is beyond the scope of this chapter, a fair approximation of the basic

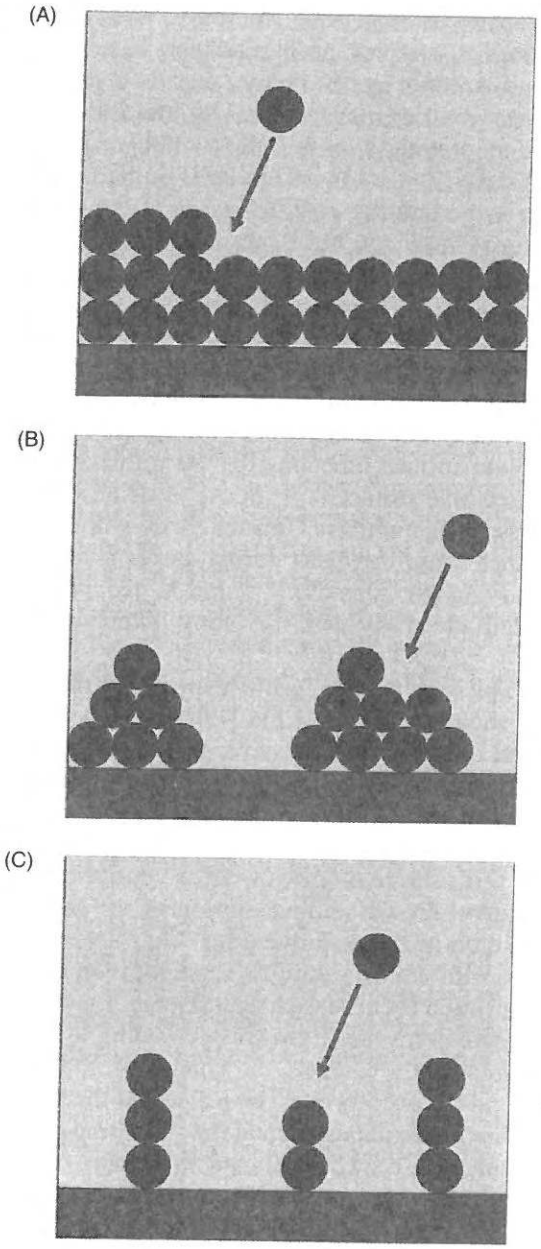

Figure 4.13 Illustration of differences in adsorption growth behavior. (A) Near sequential formation of one layer after another due to preference for lateral (edge to edge) growth classed as Frank–van der Merwe-type growth. (B) Island formation adsorption behavior (also known as Volmer–Weber adsorption) due to similar preferences for lateral and vertical growth modes. (C) Columnar growth behavior resulting from strong preference for vertical growth modes only.

n growth behavior. (A) Near another due to preference for s Frank–van der Merwe-type on behavior (also known as ar preferences for lateral and owth behavior resulting from des only.

behavior of all three preceding types can be arrived at on the back of the following simplifications:

1. The first adsorption layer is allowed to form lateral interactions (cluster formation as described in the previous sections).
2. Deposition of solute to the primary adsorptive surface to form the first surface layer is considered chemically distinct from adsorption to any other surface layer, *i.e.* $(k_1)_{\{L1\}} \neq (k_1)_{\{LY\}}$, where Y denotes an adsorbate layer greater than 1, *i.e.* $Y>1$.
3. Deposition on top of the first adsorbed surface layer is {L2} chemically equivalent to deposition on any other higher layer ({L3},{L4} . . .), *i.e.* $(k_1)_{\{LY\}} = (k_1)_{\{LW\}}$, where $Y>1$ and $W>1$.
4. The total surface area available for adsorption to a particular multilayer, $A_{tot\{LY\}}$ above the first layer (i.e. {LY} for $Y>1$) at any stage of the experiment is equal to $\phi_{\{L(Y-1)\}}A_{tot\{L1\}}$. This statement is equivalent to saying that there can be no unsupported growth. The remaining free surface area not covered by adsorbate on the first layer is equal to $(1-\phi_{\{L1\}})A_{tot\{L1\}}$.
5. Surface functions for each layer of growth are calculated on the basis of an assumed continuous surface area.[31]

On the back of the preceding postulates the set of rate equations describing the adsorption rate to the first layer can be written using either Eq. set 4.27 or 4.31 and then used again to express the rate of adsorption to each particular layer above the first, using Eq. set 4.31.

4.3 Summary and Conclusions

The study of adsorption and interfacial phenomena is indeed a very important subject in biology. Table 4.1 describes some of the essential roles that adsorption phenomena play in the fundamental processes of life. In this chapter, we have examined how adsorption phenomena can be studied using optical biosensor technology. After discussing pertinent features of the optical biosensor measurement technique, we examined some of the physical chemistry behind the process of adsorption. We formalized our discussion of adsorption by breaking it down into its component pieces. We covered the process of mass transfer to the surface and looked at how under some circumstances this could be rate limiting. Under conditions in which mass transfer effects are negligible, we described how the form of the adsorption progress curve would be determined by differences in the adsorption mechanism. We further deconstructed our analysis of adsorption mechanism into two separate discussions. The first

[31] Obviously this assumption will be weak when the preceding layer is not clustered and in this case so-called "edge effects" will play some role. However, as the degree of cluster formation becomes greater the assumption will become stronger.

concerned itself with different modes of idealized partition at zero adsorbate concentration. Here, we reviewed several fundamental types of adsorption/partition including homogeneous concerted, homogeneous stepwise and heterogeneous concerted and stepwise modes. In the second discussion, we examined how each new adsorbate addition would affect the likelihood of the next adsorbate addition. We then introduced and reviewed the different forms that the surface function[32] may take for different types of adsorption events. By extension, we examined how both attractive and repulsive interactions between adsorbate molecules or between adsorbate and intimate solute molecules would affect such surface functions. We also examined the effect on the surface function of multilayer growth and introduced some of the basic modes that such multilayer growth might take.

Many reviews tend to focus on adsorption mechanisms in the absence of mass transport considerations or alternately put their focus on mass transfer limitations while treating adsorption phenomena with overly simplistic 1:1 binding models. We feel that this review has filled a gap by providing an introduction to the general features associated with the adsorption of macromolecules to surfaces by focusing on both areas. Throughout this chapter we have tried to enter discussions from the viewpoint of a biochemist investigating biologically related adsorption phenomena involving macromolecules. In this vein, we have not concentrated on some of the typical topics more preferred by chemists such as discussions of the energetic differences between physisorption and chemisorption.[33] Equally, we presented the discussion of mass transfer effects in non-transformed quantities as opposed to the approaches preferred by the (generally) more mathematically oriented engineering community. However, with these caveats out in front we have unashamedly tried to engage the reader with some of the complexity (and wonders) associated with the biophysical approach to the study of adsorption. Interfacial events form such a part of our everyday living that it is not overly dramatic to finish this review with a line from a short poem by Vroman [82]:

"All we can create and cry is interface"

4.4 Questions

1. a. With respect to the phenomenon of adsorption define the following terms:
   - solute
   - adsorbate
   - binding/matrix site.

[32] A probability function describing the likelihood of solute finding an available site on the surface for adsorption.

[33] Distinctions which have less functional meaning when examining the non-covalent adsorption of very large molecules.

b. With respect to the natures of both the solute and matrix site, discuss what is meant by the terms:

- distinct array of binding sites
- continuum of binding sites.

2. a. Optical biosensors measure the amount of adsorbate directly, as opposed to chromatographic procedures, which measure the amount of adsorbate by calculating the difference between the total and free solute concentrations during and after adsorption. Give three advantages of such a direct measurement technique for quantifying the adsorption process.
   b. If the efficiency of detecting adsorbed solute using an optical biosensor decays exponentially with distance normal to the surface, comment on what type of adsorption reactions and adsorption geometries would be the most straightforward to categorize.
3. a. Starting with the basic transport/reaction scheme outlined in eqn. (4.4), derive the limiting case kinetic behavior for (i) transport-limited and (ii) reaction-limited adsorption.
   b. Comment on how mass transport might be accounted for in a completely general fashion regardless of tube/cell geometries.
   c. What approximate forms of the general approach given in your answer to (b) are useful for describing mass transport in a flow-through and cuvette-type biosensor?
4. a. Adsorption reaction mechanisms can be described completely generally as partition events in which the partition rate is a function of the extent and type of surface occupation. Discuss the above statement in terms of the components that constitute the association rate function k_1' [eq. (4.5)].
   b. Write down kinetic mechanisms for the following types of adsorption behavior where unless specified the adsorption is of a simple concerted type:

- adsorption of a homogeneous solute to a homogeneous array of binding sites
- multi-step adsorption pathway of a homogeneous solute to a homogeneous array of binding sites
- adsorption of heterogeneous solute to a homogeneous array of binding sites
- adsorption of homogeneous solute to a heterogeneous array of binding sites.

5. Adsorption reactions can be categorized into two general types, those capable of being saturated (*i.e.* a fixed number of adsorption sites) and those incapable of being saturated (a non-fixed number of adsorption sites, usually corresponding to multilayer formation).

a. What surface functions are applicable to the following types of saturable adsorption reactions?:

- Langmuir adsorption
- irreversible adsorption of spherical solute to a continuum array of binding sites
- reversible adsorption of spherical solute to a continuum array of binding sites
- reversible adsorption of spherical solute to a continuum array of binding sites with adsorbate clustering leading to monolayer formation.

b. Describe in general terms the differences between the three types of multilayer adsorption growth with respect to the adsorbate preference for forming lateral or longitudinal contacts with the already adsorbed solute.

6. Mass transport-limited kinetics are beneficial for concentration determination of the analyte in a sample. Why?

4.5 Symbols

$\bar{v}_i$	partial specific volume of solute
$(C_1)_{\text{ads}[i]}$	concentration of adsorbed monomer clusters on surface of size i monomers
$(C_i)_{\text{ads}}$	concentration of adsorbed solute of type i
$(C_x)_{\text{tot}}$	initial total concentration of matrix sites
$(K_i)_{\text{eff}}$	effective adsorption partition constant $[(K_i)_{\text{eff}} = f_i/b_i]$
$\{C_i\}$	concentration of solute of type i spatially close to the surface (termed intimate solute)
B	multi-term flow parameter, dependent upon device geometry
b_i	effective dissociation rate parameter
C_{BULK}	solute concentration in the bulk solution
c_i	weight concentration of component i
C_i	concentration of solute of type i
c_v	weight concentration of viscogenic agents
D_i	solute's diffusion coefficient
ΔE_c	stabilizing energy (in cluster formation)
F	forward rate constant (units of s^{-1})
ΔS	change in signal
ϕ	fractional site/area coverage
$\phi_{\max}$	maximal adsorbate site coverage
$f(\phi)$	unitless function describing the surface site occupation, where $\Phi = n(Ci)\text{ads}/(Cx)\text{tot}$ (here n is the average number of sites covered by the adsorbed solute)
$f_3(\phi_{1a},\phi_{1b})$	stepwise specific surface function, describes the fractional availability of nearby matrix sites
f_i	effective forward rate parameter

η	aqueous solvent of viscosity
i	component i
k	Boltzmann's constant
k_1	intrinsic second-order rate constant
k_1'	association rate function (unit: s^{-1})
k_2	dissociation rate const (unit: s^{-1})
k_3	second-order rate constant (units of l mol^{-1} s^{-1})
k_a	phenomenological transport coefficient
k_b	phenomenological transport coefficient
$k_{3[i]}$	intrinsic association rate constant for clusters of size i on the surface
$k_{4[i]}$	intrinsic dissociation rate constant for clusters of size i on the surface
K_R'	$K_R' = k_1'/k_2$
K_T	partition constant for formation of the intimate solute
M_i	solute i molecular weight
n	refractive index
N_A	Avogadro's number
n_i	average number of matrix sites occupied by adsorbate i
S	signal (optical)
T	temperature
v^*	average velocity of liquid in flow cell
v_{BULK}	velocity of the bulk of the liquid
v_i	linear velocity of solute
v_x	linear velocity in the x direction
z	axis normal to the sensor surface
z_{max}	max height of flow channel
ρ_x	volume density of matrix sites (molecules m^{-3})
ρ_x^*	area density of matrix sites (molecules m^{-2})
σ	decay constant (unit: distance)
Δr	radius of cylindrical polymer rods
φ	fractional volume occupation of polymer
δ	small distance, the zero flow region extends out a surface

4.6 Acknowledgements

From my time in the U.K. I would like to thank Professor Christopher M. Dobson for providing me with space to work in his laboratory, his keen interest in my research and his continued friendship. During this period I would like to acknowledge the financial support of the Human Frontiers Science Program (HFSP) which financed my stay at the Cambridge University Chemical Laboratories (2003–2007) *via* the award of a HFSP Long Term Fellowship. From my time in Japan I would like to thank Professor Haruki Nakamura and Assoc. Professor Fumio Arisaka for the amazing support which they have

provided me and for which I am deeply indebted. I would like to acknowledge financial assistance from a RIKEN grant for 'Research and Development of Next-Generation Integrated Life Simulation Software.' Finally I am deeply appreciative of the valuable assistance provided by Dr. N. Hirota.

References

1. A.E. Johnson, *Traffic*, 2005, **6**, 1078.
2. I. Mellman and G. Warren, *Cell*, 2000, **100**, 99.
3. M.B. Neiditch, M.J. Federle, A.J. Pompeani, R.C. Kelly, D.L. Swemm, P.D. Jeffrey, B.L. Bassler and F.M. Hughson, *Cell*, 2006, **126**, 1095.
4. K.A. Janes, J.G. Albeck, S. Gaudet, P.K. Sorger, D.A. Lauffenburger and M.B. Yaffe, *Science*, 2005, **310**, 1646.
5. W. Cho and R.V. Stahelin, *Annu. Rev. Biophys. Biomol. Struct.*, 2005, **34**, 119.
6. K. Kristiansen, *Pharmacol. Ther.*, 2004, **103**, 21.
7. R. Benton, *Cell. Mol. Life. Sci.*, 2006, **63**, 1579.
8. J.R. Pugh and I.M. Raman, *Biophys. J.*, 2005, **88**, 1740.
9. J. McGhee and P. von Hippel, *J. Mol. Biol.*, 1974, **86**, 469.
10. A.A. Aderem and D.M. Underhill, *Annu. Rev. Immunol.*, 1999, **17**, 593.
11. S. Abraham, S. Brahim, K. Ishihara and A. Guiseppi-Elie, *Biomaterials*, 2005, **26**, 4767.
12. R.J. Green, M.C. Davies, C.J. Roberts and S.J. Tendler, *J. Biomed. Mater. Res.*, 1998, **42**, 165.
13. D.J. Winzor and W.E. Sawyer, *Quantitative Characterization of Ligand Binding*, Wiley-Liss, New York, 1995.
14. L. Gorton (Ed.), *Biosensors and Modern Specific Biospecific Analytical Techniques*, in *Comprehensive Analytical Chemistry*, Series Ed. D. Barcelo, Elsevier, Amsterdam, 2005, p. xliv.
15. J. Fraden, *Handbook of Modern Sensors: Physics, Designs and Applications*, Springer, New York, 2004.
16. M. Terpstra, *Biosens. Bioelectron.*, 1993, **8**, ii.
17. R. Cush, J.M. Cronin and J.M. Stewart, *Biosens. Bioelectron.*, 1993, **8**, 347.
18. U. Jonnson, L. Fagerstram and B. Ivarsson, *Biotechniques*, 1999, **11**, 620.
19. F. de Fornel, *Evanescent Waves: From Newtonian Optics to Atomic Optics*, Springer-Verlag, Berlin, 2001, p. 1.
20. H. Raether, in *Physics of Thin Films*, G. Haas, M.H. Francombe and R.W. Hoffmann (Eds.), Vol. 9, Academic Press, New York, 1977, p. 145.
21. D. Shoup and A. Szabo, *Biophys J.*, 1982, **40**, 33.
22. L. Edelstein-Keshet, *Mathematical Models in Biology*, SIAM, Philadelphia, PA, 2005.
23. H.C. Berg, *Random Walks in Biology*, Princeton University Press, New Jersey, 1993, Chap. 3.
24. R.C. Weast (Ed.), *CRC Handbook of Chemistry and Physics*, 62nd edn., CRC Press, Boca Raton FL, 1981, Table F42.

. I would like to acknowledge
esearch and Development of
ftware.' Finally I am deeply
by Dr. N. Hirota.

99.
i, R.C. Kelly, D.L. Swemm,
ı, *Cell*, 2006, **126**, 1095.
ger, D.A. Lauffenburger and

ys. Biomol. Struct., 2005, **34**,

21.
79.
5, **88**, 1740.
1974, **86**, 469.
v. Immunol., 1999, **17**, 593.
Guiseppi-Elie, *Biomaterials*,

J. Tendler, *J. Biomed. Mater.*

Characterization of Ligand

pecific Biospecific Analytical
nistry, Series Ed. D. Barcelo,

ics, Designs and Applications,

ns. Bioelectron., 1993, **8**, 347.
Biotechniques, 1999, **11**, 620.
nian Optics to Atomic Optics,

laas, M.H. Francombe and
ss, New York, 1977, p. 145.
, 33.
Biology, SIAM, Philadelphia,

eton University Press, New

stry and Physics, 62nd edn.,

25. S. Uribe and J.G. Sampedro, *Biol. Proc. Online*, 2003, **5**, 103.
26. A.G. Ogston, B.N. Preston and D.J. Wells, *Proc. R. Soc. London A*, 1973, **333**, 297.
27. A. Pluen, P.A. Netti, R.K. Jain and D.K. Berk, *Biophys. J.*, 1999, **77**, 542.
28. V.G. Levich, *Physicochemical Hydrodynamics*, Prentice Hall, Englewood Cliffs, NJ, 1962.
29. R.B. Bird, W.E. Stewart and E.N. Lightfoot, *Transport Phenomena*, Wiley, New York, 1960.
30. R.W. Glaser, *Anal. Biochem.*, 1993, **213**, 152.
31. P. Schuck, *Biophys. J.*, 1996, **70**, 1230.
32. M.L. Yarmush, D.B. Patankar and D.M. Yarmush, *Mol. Immunol.*, 1996, **33**, 1203.
33. D.G. Myszka, X. He, M. Dembo, T.A. Morton and B. Goldstein, *Biophys. J.*, 1998, **75**, 83.
34. C. Wofsy and B. Goldstein, *Biophys. J.*, 2002, **82**, 1743.
35. M. Elimelech, X. Jia, J. Gregory and R. Williams, *Particle Deposition and Aggregation: Measurement, Modelling and Simulation*, Butterworth Heinemann, London, 1998.
36. D.A. Edwards, *SIAM J.*, 2000, **105**, 1.
37. P. Schuck and A.P. Minton, *Anal. Biochem.*, 1996, **240**, 262.
38. R. Karlsson, H. Roos, L. Fagerstram and B. Persson, *Methods Comp. Methods Enzymol.*, 1994, **6**, 99.
39. J. Witz, *Anal. Biochem.* 1999, 270, 201.
40. B.K. Lok, Y.L. Cheng and C.R. Robertson, *J. Colloid Interface Sci.*, 1983, **91**, 104.
41. S. Sjolander and C. Urbaniczky, *Anal. Chem.*, 1991, **63**, 2338.
42. D. Hall, *Anal. Biochem.*, 2001, **288**, 109.
43. P. Schuck, *Annu. Rev. Biophys. Biomol. Struct.*, 1997, **26**, 541.
44. D.G. Myszka, T.A. Morton, M.L. Doyle and I.M. Chaiken, *Biophys. Chem.*, 1997, **64**, 127.
45. R. Karlsson and A. Falt, *J. Immunol. Methods*, 1997, **200**, 121.
46. C. Calonder and P.R. Van Tassel, *Langmuir*, 2001, **17**, 4392.
47. W.H. Press, S.A. Teukolsky, W.T. Vetterling and B.P. Flannery, *Numerical Recipes in C*, Cambridge University Press, Cambridge, 2002.
48. T.M. Morton, D.G. Myszka and I.M. Chaiken, *Anal. Biochem.*, 1995, **227**, 176.
49. K.M. Müller, K.M. Arndt and A. Plückthun, *Anal. Biochem.*, 1998, **261**, 149.
50. N.L. Kalinin, L.D. Ward and D.J. Winzor, *Anal. Biochem.*, 1995, **228**, 238.
51. P.R. Van Tassel, L. Guemouri, J.J. Ramsden, G. Tarjus, P. Viot and J. Talbot, *J. Colloid Interface Sci.*, 1998, **207**, 317.
52. J. Svitel, A. Balbo, R.A. Mariuzza, N.R. Gonzales and P. Schuck, *Biophys. J.*, 2003, **84**, 4062.
53. L. Vroman, A.L. Adams and M. Klings, *Fed. Proc.*, 1971, **30**, 1494.
54. P. Schaaf, J. Voegel and B. Senger, *J. Phys. Chem. B*, 2000, **104**, 2204.
55. P. Schaaf and J. Talbot, *Phys. Rev. Lett.*, 1989, **62**, 175.

56. I. Lundstrom, *Prog. Colloid Polym. Sci.*, 1985, **70**, 76.
57. R.C. Chatelier and A.P. Minton, *Biophys. J.*, 1996, **71**, 2367.
58. P. Wojciechowski and J.L. Brash, *J. Colloid Interface Sci.*, 1989, **140**, 239.
59. S. Stankowski, *Biochim. Biophys. Acta*, 1983, **735**, 352.
60. A.W. Adamson, in *Physical Chemistry of Surfaces*, Wiley, New York, 1982, Chapter 16.
61. T.J. Halthur, A. Bjorklund and U.M. Eloffson, *Langmuir*, 2006, **22**, 2227.
62. D.R. Hall, N.N. Gorgani, J.G. Altin and D.J. Winzor, *Anal. Biochem.*, 1997, **253**, 145.
63. I. Langmuir, *J. Am. Chem. Soc.*, 1918, **40**, 1361.
64. J.J. Ramsden, G.I. Bachmanova and A.I. Archakov, *Phys. Rev. E*, 1994, **50**, 5072.
65. H. Reiss, H.L. Frisch and J.L. Lebowitz, *J. Chem. Phys.*, 1959, **31**, 369.
66. J.L. Lebowitz, E. Helfland and E. Praestgaard, *J. Chem. Phys.*, 1965, **43**, 774.
67. M.C. Bartelt and V. Privman, *Int. J. Mod. Phys.*, 1991, **5**, 2883.
68. J.W. Evans, *Rev. Mod. Phys.*, 1983, **65**, 1281.
69. P.L. Krapivsky and E. Ben-Naim, *J. Chem. Phys.*, 1995, **100**, 6778.
70. X. Jin, G. Tarjus and J. Talbot, *J. Phys. A*, 1994, **27**, L195.
71. D. Hall, Optical Biosensor Based Studies of Protein, Adsorption: Theory and Measurement, *PhD Thesis*, University of Queensland Press, Brisbane, 2000.
72. A.P. Minton, *Biophys. J.*, 1999, **76**, 176.
73. P.G. Vekilov and J.I.D. Alexander, *Chem. Rev.*, 2000, **100**, 2061.
74. D.D. Vvdensky, A. Zangwill, C.N. Luse and M.R. Wilby, *Phys. Rev. E*, 1993, **48**, 852.
75. F.A. Ponce and D.P. Bour, *Nature*, 1997, **386**, 351.
76. U.G. Volkmann and K. Knorr, *Phys. Rev. Lett.*, 1991, **66**, 473.
77. J. Texter and M. Tirrell, *AIChE J.*, 2001, **47**, 1706.
78. S. Brunauer, P.H. Emmett and E. Teller, *J. Am. Chem. Soc.*, 1938, **60**, 309.
79. F.C. Frank and J.H. van der Merwe, *Proc. R. Soc. London, Ser. A*, 1949, **198**, 205.
80. M. Volmer and A. Weber, *Z. Phys. Chem.*, 1926, **119**, 277.
81. G.S. Bales and A. Zangwill, *J. Vac. Sci. Technol.*, 1991, **9**, 145.
82. As quoted by J.D. Andrade, in *Surface and Interfacial Aspects of Biomedical Polymers*, Plenum Press, New York, 1985, Preface to Vol. 1.